AD-A185 140 PREPARATION OF FINE OXIDE POWDERS BY EMULSION PRECIPITATION(U) IOWA STATE UNIV AMES M AKINC 31 MAY 87 ARO-21718 3-MS DAAG29-85-K-0086 1/1

UNCLASSIFIED F/G 11/2 NL

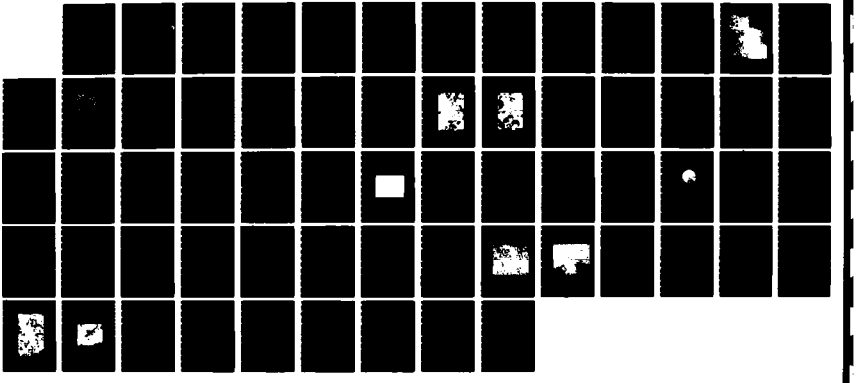

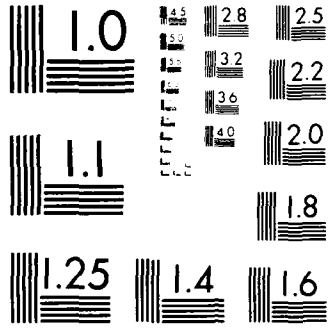

MICROCOPY RESOLUTION TEST CHART
NATIONAL BUREAU OF STANDARDS 1963-A

ARO 21718.3-MS

(2)

Preparation of Fine Oxide Powders by Emulsion Precipitation

Final Report
by
Mufit Akinc, Ph.D.
Iowa State University

May 31, 1987

Prepared for
U.S. Army Research Office
Research Triangle Park NC 27709
Contract #: DAAG29-85-K-0086

REPORT DOCUMENTATION PAGE

1a. REPORT SECURITY CLASSIFICATION Unclassified AD-A185140	1b. RESTRICTIVE MARKINGS
2a. SECURITY CLASSIFICATION AUTHORITY	3. DISTRIBUTION / AVAILABILITY OF REPORT Approved for public release; distribution unlimited.
2b. DECLASSIFICATION / DOWNGRADING SCHEDULE	
4. PERFORMING ORGANIZATION REPORT NUMBER(S)	5. MONITORING ORGANIZATION REPORT NUMBER(S) ARO 21718.3-MS
6a. NAME OF PERFORMING ORGANIZATION Iowa State U of Sci & Tech 6b. OFFICE SYMBOL (*If applicable*)	7a. NAME OF MONITORING ORGANIZATION U. S. Army Research Office
6c. ADDRESS (*City, State, and ZIP Code*) Ames, Iowa 50011-2522	7b. ADDRESS (*City, State, and ZIP Code*) P. O. Box 12211 Research Triangle Park, NC 27709-2211
8a. NAME OF FUNDING / SPONSORING ORGANIZATION U. S. Army Research Office 8b. OFFICE SYMBOL (*If applicable*)	9. PROCUREMENT INSTRUMENT IDENTIFICATION NUMBER DAAG29-85-K-0086
8c. ADDRESS (*City, State, and ZIP Code*) P. O. Box 12211 Research Triangle Park, NC 27709-2211	10. SOURCE OF FUNDING NUMBERS PROGRAM ELEMENT NO. / PROJECT NO. / TASK NO. / WORK UNIT ACCESSION NO.

11. TITLE (*Include Security Classification*)
Preparation of Fine Oxide Powders by Emulsion Precipitation

12. PERSONAL AUTHOR(S)
Mufit Akinc

13a. TYPE OF REPORT	13b. TIME COVERED	14. DATE OF REPORT (*Year, Month, Day*)	15. PAGE COUNT
Final	FROM 4/14/85 TO 4/14/87	1987, May 31	56

16. SUPPLEMENTARY NOTATION
The view, opinions and/or findings contained in this report are those of the author(s) and should not be construed as an official Department of the Army position, policy, or decision, unless so designated by other documentation.

17 COSATI CODES		
FIELD	GROUP	SUB-GROUP

18. SUBJECT TERMS (*Continue on reverse if necessary and identify by block number*)
Emulsion Precipitation, Fine Oxide Powders, Oxide Systems Oxide Powders, Ceramic Oxide Powders, Emulsifying Agents,

19. ABSTRACT (*Continue on reverse if necessary and identify by block number*)

This program has centered on the preparation of fine ceramic oxide powders by a new method called Emulsion Precipitation. The main emphasis of the investigation was given to understanding the influence of emulsion characteristics on the morphology of the powders produced. It was found that the method proposed does, in fact, produce powders of submicron size and spherical shape for a relatively broad range of experimental conditions.

20. DISTRIBUTION / AVAILABILITY OF ABSTRACT ☐ UNCLASSIFIED/UNLIMITED ☐ SAME AS RPT. ☐ DTIC USERS	21. ABSTRACT SECURITY CLASSIFICATION Unclassified
22a. NAME OF RESPONSIBLE INDIVIDUAL	22b. TELEPHONE (*Include Area Code*) / 22c. OFFICE SYMBOL

ARO 21718.3-MS

20. ABSTRACT CONTINUED

During the course of the investigations, the influence on characteristics of the powders of composition of the organic phase, the emulsifying agent, and the aqueous phase was studied. It was shown that, by following optimum processing procedures, nearly monosize (0.1 - 0.2 μm), spherical powders can be produced reproducibly. It was also shown that the method is applicable to a variety of single and multicomponent oxide systems.

TABLE OF CONTENTS

The views, opinions, and/or findings contained in this report are those of the author(s) and should not be construed as an official Department of the Army position, policy, or decision, unless so designated by other documentation.

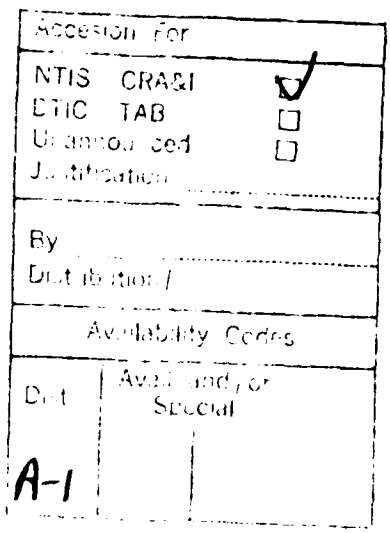

FOREWORD

This program has centered on the preparation of fine ceramic oxide powders by a new method called Emulsion Precipitation. The main emphasis of the investigation was given to understanding the influence of emulsion characteristics on the morphology of the powders produced. It was found that the method proposed does, in fact, produce powders of submicron size and spherical shape for a relatively broad range of experimental conditions.

During the course of the investigations, the influence on characteristics of the powders of composition of the organic phase, the emulsifying agent, and the aqueous phase was studied. It was shown that, by following optimum processing procedures, nearly monosize (0.1 - 0.2 μm), spherical powders can be produced reproducibly. It was also shown that the method is applicable to a variety of single and multicomponent oxide systems.

This final report contains a summary of the major accomplishments, as well as some of the new findings that were not included in the progress reports and publications that were previously submitted to ARO.

STATEMENT OF PROBLEM STUDIED

During the course of this project a new method (Emulsion Precipitation) for producing fine, unagglomerated oxide powders was investigated. The main goal of the study was to demonstrate the viability of the technique and to investigate the influence of various organic phase, emulsifying agent and aqueous phase compositions.

The first part of the work (first year) was focused on preparation and characterization of emulsions with respect to type of emulsion formed, average droplet size and size distribution, and stability of the emulsion as a function of time and temperature. A number of organic liquids, emulsifiers and aqueous solutions were employed at different volume ratios to produce a 'working' compositional map of emulsions that could be used for powder preparation.

In the second part of the project (second year), powders were produced from the emulsions that were deemed to be suitable for processing. Precursor powders are produced by either i) the emulsion evaporation technique, or ii) the emulsion precipitation technique. The effects of process variables on powder particle morphology and on process yield were investigated. The sintering behavior of these powders was also studied, and the sintered densities of compacts produced with the emulsion technique were compared to those produced from commercial powders.

1. INTRODUCTION

This program is concerned with developing a new method for production of fine ceramic oxide powders from emulsions. Previous studies in our laboratory, as well as elsewhere, had shown that a number of variables in the chemical precipitation-drying-calcination route drastically affect the physical state of the powders produced (1-4). Among the more important findings are that precipitation direction, final pH of the suspension and the way the water is removed from the precipitate control the primary particle size, degree of agglomeration and the strength of the agglomerates formed. The main goal of the present work was to demonstrate formation of uniform, fine particle size oxide powders by using small aqueous droplets of a water-in-oil (w/o) emulsion as the precipitation medium. Using this approach, it was predicted that the size of the primary particles (or agglomerates) would be limited to the emulsion droplet size (5).

The present report discusses the recent progress made on formation and characteristics of oxide powders, specifically yttria, made by the emulsion route. This work has demonstrated clearly that the new technique is a viable method for producing a variety of single and multicomponent oxides, and that it holds promise for the production of non-oxide materials, such as sulfides. This program has reached a point where the research should be directed toward investigation of the mechanism of particle formation. In addition, broadening the application of this technique to a encompass a number of chemically-diverse systems is recommended.

2. RESULTS

2.A. EMULSIONS

Numerous emulsions were prepared in order to select a working emulsion composition for powder preparation experiments. Toluene, benzene, hexane, kerosene, mineral oil and paraffin oil were investigated as organic liquids Water-in-oil (w/o) type emulsions were successfully produced from all of these non-polar organics. In the preliminary experiments, a large number of anionic and non-ionic commercial emulsifying agents were tried, including Aerosol-OT, Arlacel 83, Span 60, Span 80, Tween 80, Tween 85, Pluronic L62 and Pluronic L102. The emulsifying agents with an HLB value between 3 and 10 usually exhibited w/o type emulsions with varying degrees of stability, as will be discussed below. Distilled water aqueous solutions of Y^{+3}, Mg^{++} or Al^{+3} in the 0.2 to 4.0 M concentration range were employed as dispersed phase. During the course of the study, it was observed that anionic surfactants such as Aerosol-OT produced stable w/o emulsions with distilled water as the internal phase, but these emulsions became unstable in the presence of cations. However, nonionic surfactants were found to show good stability in the presence of cations (6). Emulsions made with nonionic surfactants were quite stable up to the boiling point of the aqueous solution, while those made with Aerosol-OT phase separated when the temperature of the emulsion was raised above room temperature. Therefore, anionic emulsifying agents were discarded in favor of nonionic agents for the remainder of this work. For the emulsion precipitation experiments, toluene and benzene were chosen as organic phases, because they provided the best diffusivity medium for the precipiting bases. Kerosene and mineral oil were used for the emulsion evaporation studies, as these organics have significantly higher boiling points than the aqueous phase.

2.A.1. Emulsion Composition

Emulsifier concentration and aqueous phase volume content of the emulsions were found to influence the stability and the average droplet size of the emulsions prepared. For example, emulsion characteristics of toluene/aqueous 0.44M $Y(NO_3)_3$/Span 60 compositions are summarized in Table 1.

Table 1. Stability and droplet size of w/o emulsions in toluene/aqueous 0.44M $Y(NO_3)_3$/Span 60 system.

Emulsion Designation	Composition v/o Toluene	Aqueous	Span 60	Characteristics Stability	Size, μm
A1	74.0	25.0	1.0	stable	4-40
A2	73.5	24.5	2.0	stable	4-32
A3	72.0	24.0	4.0	stable	1-20
A4	70.5	23.5	6.0	stable	1-20
A5	69.0	23.0	8.0	stable	1-10
B1	74.0	25.0	1.0	stable	4-40
B2	59.0	39.4	1.6	stable	8-70
B3	49.0	49.0	2.0	stable	8-130
B4	39.0	58.4	2.6	not stable	
B5	24.0	73.0	3.0	not stable	

In series A, the aqueous-to-organic phase ratio was kept constant and emulsifier concentration was varied; in series B, the aqueous phase-to-emulsifier ratio was kept constant but organic phase content was decreased. Table 1 and Figure 1 show that, as the emulsifier concentration increased, the droplet size decreased, and as the organic phase content decreased, the droplet size increased. In fact, when the aqueous phase content was increased beyond 50 v/o, the emulsions exhibited irregular droplet shape and became unstable. When the emulsions were subjected to sonic disruption droplet size was reduced to submicron range. However, especially in high aqueous phase volume ratios extensive agglomeration was evident.

A number of nonionic emulsifiers were tried, to select a proper emulsifier for higher boiling point organic liquids such as mineral oil, paraffin oil and kerosene. For these experiments a relatively large quantity (10 v/o) of emulsifier was employed. Table 2 shows that Span 80, Span 85 and Arlacel 83 produce w/o type emulsion with all three organic liquids, while other o/w or w/o type emulsions are produced by Tween 80 and Tween 85, depending upon the organic phase. The influence of the organic phase on the type of emulsion formed for different emulsifiers is not clearly understood, however, it is probably related to the solubility of the emulsifiers in the organic phase. In general, it was found that emulsifiers with an HLB value of 4 to 11 formed relatively stable w/o type emulsions. Because w/o type emulsions could be readily produced with certain common emulsifiers, further investigation of this influence were not deemed within the scope of the present study.

Although the method of stirring did not seem to alter the type of emulsions formed, it had a drastic effect on the droplet size. Mechanical stirring of the emulsions produced droplets of tens of microns to about one micron

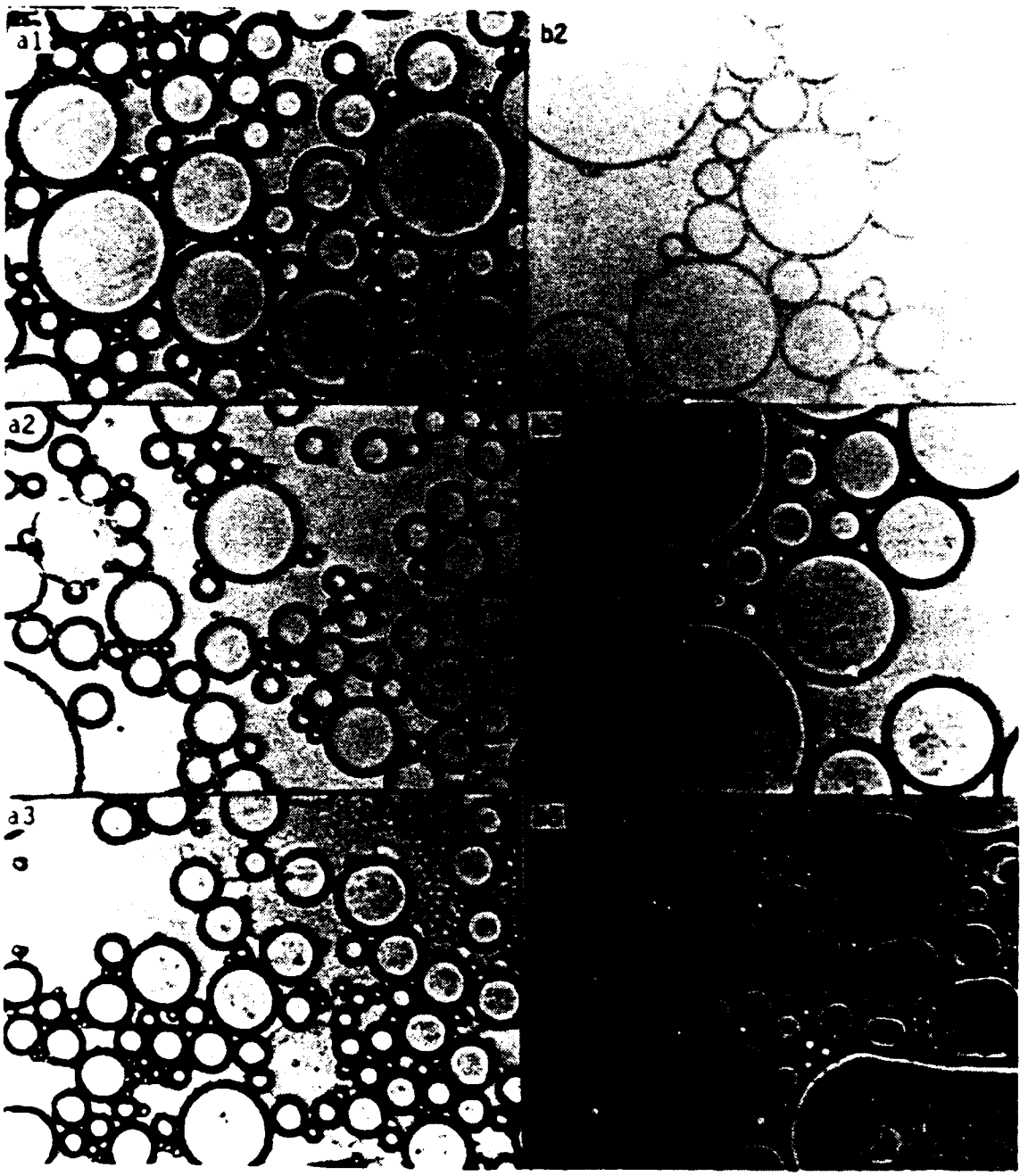

Fig. 1. Variation of droplet size and distribution in w/o type emulsions. Compositions of emulsions are given in Table 1.

Table 2. Characteristics of emulsions prepared by higher boiling point organics and non-ionic emulsifiers.

Emulsifier		Organic Phase: Mineral Oil	Paraffin Oil	Kerosene
SPAN 85	Type	w/o	w/o	w/o
HLB = 1.8	Stability	separates in one hour	viscous and stable	separates in 15 minutes
	Droplet size, μm	5 - 45	5 - 40	1 - 15
SPAN 80	Type	w/o	w/o	w/o
HLB = 4.3	Stability	stable one day	stable	separates in one hour
	Droplet size, μm	2 - 30	1 - 10	1 - 50
ARLACEL	Type	w/o	w/o	w/o
HLB = 3.7	Stability	stable one hour	stable	separates quickly
	Droplet size, μm	1 - 15	1 - 15	*
TWEEN 85	Type	o/w	o/w	w/o
HLB = 11	Stability	viscous	viscous	stable for 8 hours
	Droplet size, μm	*	*	1 - 5
TWEEN 80	Type	w/o	o/w	o/w
HLB = 15	Stability	very viscous	viscous	viscous
	Droplet size, μm	5 - 40	*	*

* not applicable.

size, depending on the aqueous phase content and the duration of stirring. A typical emulsion composition of 72 v/o toluene; aqueous 25 v/o 0.4M $Y(NO_3)_3$ and 3 v/o emulsifier (1.6 Span 60 + 1.4 Tween 80), which was stirred for 15 minutes with a magnetic stirrer, showed a droplet size ranging between 4 and 40 μm. An optical micrograph of the emulsion is shown in Figure 2. The mean droplet size of this emulsion was estimated from the micrographs to be around 10-15 μm. Additional stirring of the emulsion resulted in a smaller mean size and a narrowing of the size distribution of the droplets. The droplet size distribution of the same emulsion after 10 hours of stirring is shown in Figure 3. This emulsion showed a median droplet size around 5 μm, and 90% of the droplets were within the 1 to 10 μm size range. Mean droplet diameter of this emulsion was 3 μm. Obviously, a longer agitation of the emulsion did not only reduced the mean droplet size but also resulted in more uniformly-sized droplets.

The change in mean droplet size with stirring times up to 10 hours was and is studied and shown in Figure 4. The mean droplet size decreased from about 16 μm to about 4 μm in the first two hours but only slightly after that. Obviously these values are for comparison only, as the emulsion volume, stirring speed, and size of the stirring bar all have a pronounced effect on the size of the droplets. A rather broad range of mean droplet sizes was provided by adjusting the stirring rate and stirring time. For smaller droplet sizes, sonic treatment was found to be very effective. A 10 minute sonic treatment of the emulsion (after stirring) reduced the mean droplet size from 16 μm to less than one micron; however, the size remained rather constant for additional sonic treatment up to one hour. These findings are in good agreement with literature reports that disruption of particles or droplets is instantaneous provided that the whole volume of the dispersion is exposed to cavitation (7). The ultimate size of the droplets obtained by sonic treatment is determined by the resonance frequency of the transducer. As the frequency of the transducer increased the mean droplet size decreases.

2.A.2. Emulsion Stability

The change in mean droplet size upon standing was determined in order to assess the time stability for emulsions prepared by sonic treatment. The results are plotted in Figure 5, which shows that the stability of emulsions at room temperature was quite good, with mean droplet size only increasing from 0.4 μm to 0.7 μm over

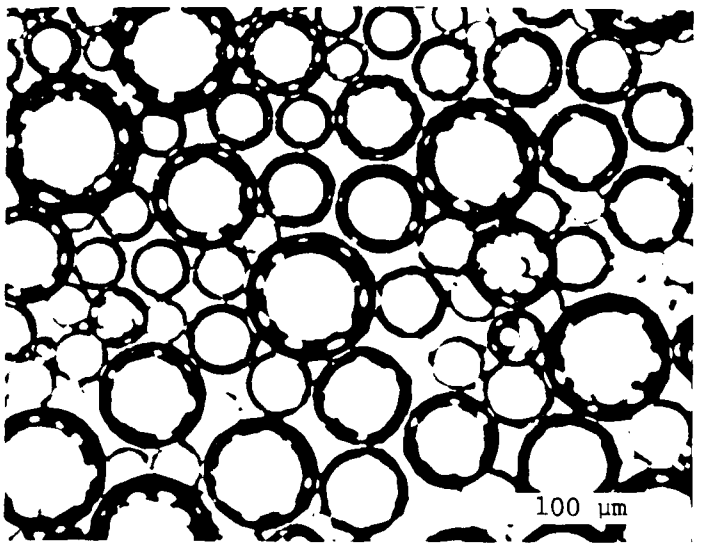

Fig. 2. Optical micrograph of emulsion prepared by 15 minutes of magnetic stirring at a low stirring speed. Emulsion composition: 72% Toluene, 25% Aqueous 0.4M $Y(NO_3)_3$ and 3% Emulsifier (1.6% Span 60 + 1.4% Tween 80).

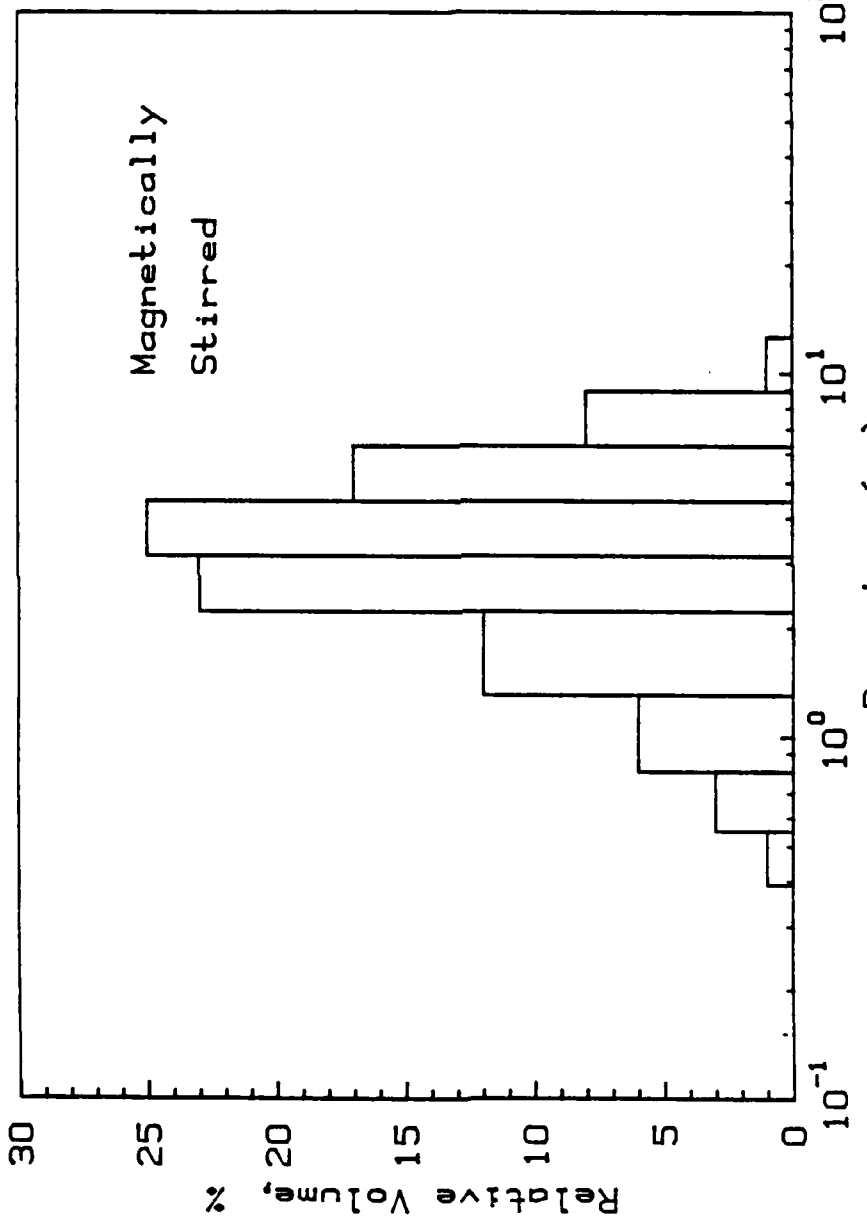

Fig. 3. Droplet size distribution of emulsion after 10 hours of mild agitation. Emulsion composition is same as in Fig. 2.

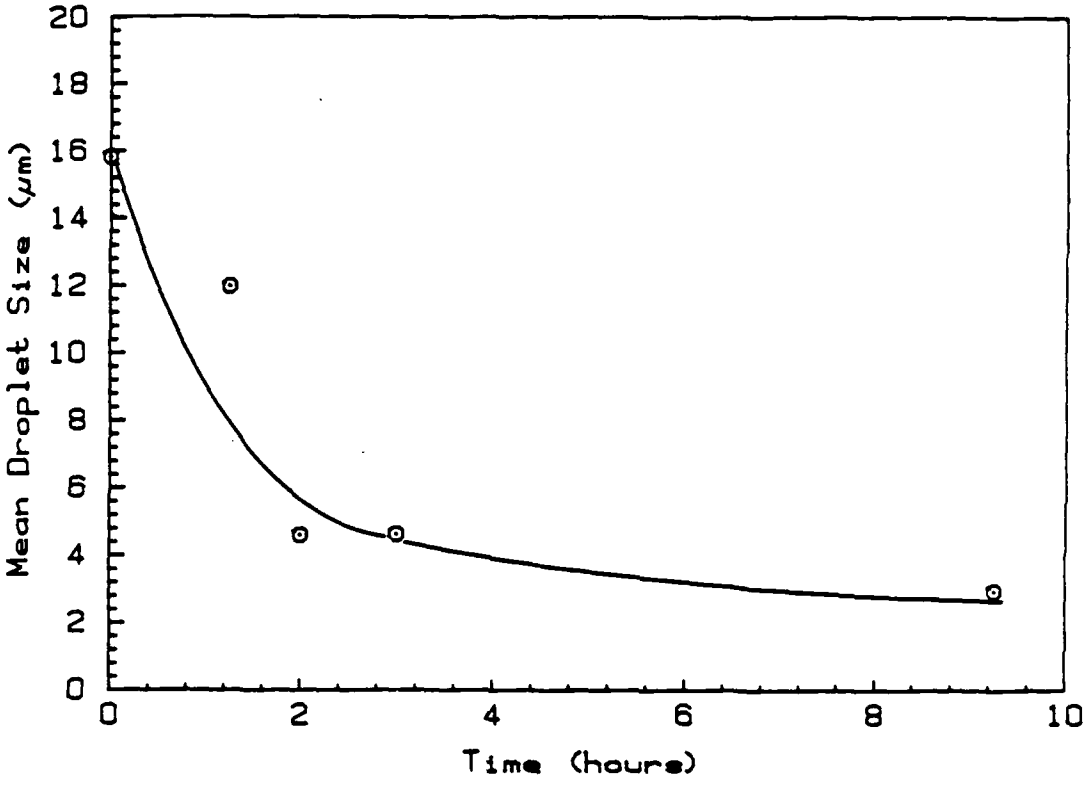

Fig. 4. Variation of mean droplet size with stirring time. Emulsions were stirred with a magnetic stirrer at a slow speed.

seven hours of standing.

The stabilities of emulsions was studied also as a function of temperature. Practically all of the emulsions that were stable at room temperature were found to be stable up to the boiling point of water. Upon cooling, most of the emulsions that were studied showed phase separation below 15°C. These results agree with previous reports (8) that the stability of w/o emulsions prepared by nonionic surfactants increases with increasing temperature.

2.B. PRECURSOR FORMATION

Two different methods for the formation of solid particles from the aqueous droplets were studied: thermal evaporation of water from the aqueous phase, which is referred to as 'emulsion evaporation' and chemical precipitation of insoluble salts within the aqueous droplets, which is referred to as 'emulsion precipitation'. Results obtained by these two methods will be discussed separately in the following sections.

2.B.1. Emulsion Evaporation

Of the various systems discussed in the emulsion section, mineral oil/aqueous $Y(NO_3)_3$/Arlacel 83 and kerosene/aqueous $Y(NO_3)_3$/Tween 85 (or Arlacel 83) were selected for emulsion evaporation studies. In these experiments, emulsions were added dropwise to a hot organic liquid having the same composition as the continuous organic phase (9), and the resulting solid particles were collected by centrifugation.

Evaporation experiments were carried out under various experimental conditions in order to assess the role of each variable on the characteristics of the powder produced. The precursor powders collected after evaporation were brown-to-black in color, amorphous and highly agglomerated due to organic residues. Upon calcination, these precursors transformed into white crystalline yttria powder.

a. Kerosene/Aqueous $Y(NO_3)_3$/Tween 85 (or Arlacel 83)

The influences of evaporation temperature and atmosphere on powder characteristics were studied from room temperature to 150°C with vacuum over the hot liquid and from 100 to 180°C with a nitrogen purge or air atmosphere over the liquid. In all cases, except at

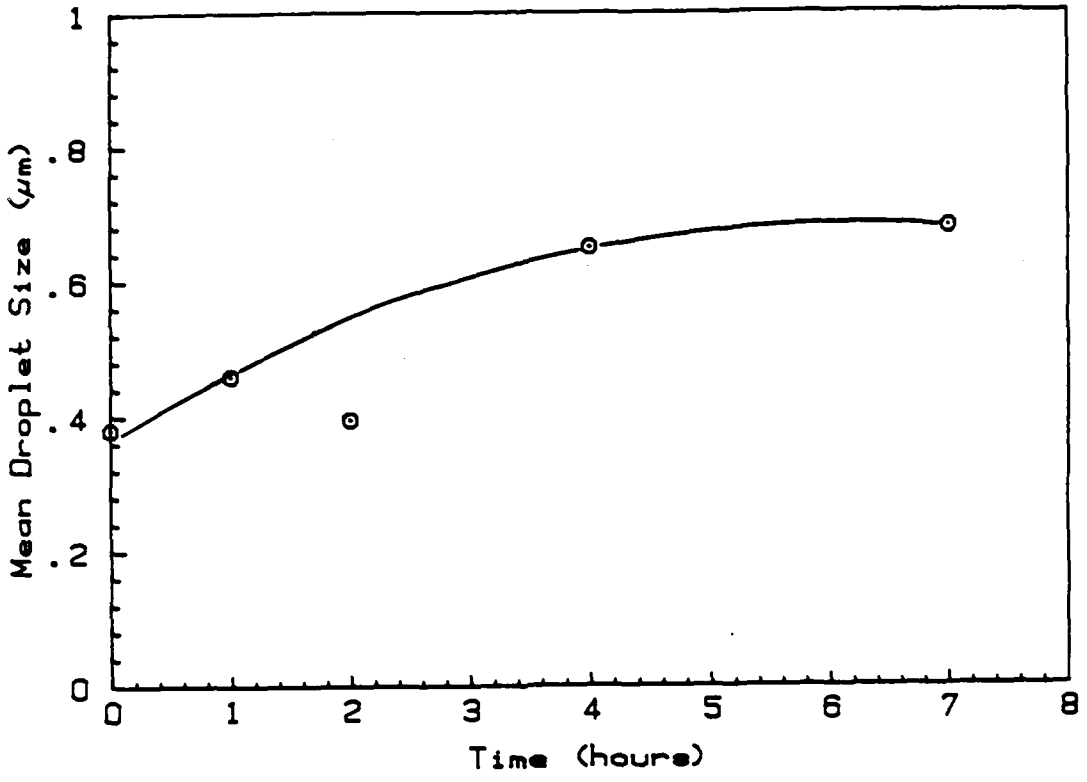

Fig. 5. Variation of mean droplet size with periods of standing for emulsions that are prepared by sonic treatment. Emulsion composition was same as that in Figure 2.

180°C, the powders exhibited unacceptable flake-like morphology. It is believed that the water evaporation rate was not high enough at the lower temperatures to transform the spherical droplets into spherical particles. Powders obtained by evaporating kerosene/aqueous 0.44M $Y(NO_3)_3$/Arlacel 83 at 180°C were submicron in size and were spherical in shape but highly agglomerated, as is shown in Figure 6.

b. Mineral Oil/Aqueous $Y(NO_3)_3$/Arlacel 83

Experiments carried out with kerosene emulsions implied that uniform particle morphologies might be possible at higher evaporation temperatures, but the boiling temperature of kerosene limited exploration of temperature regimes above 180 °C. Consequently, an organic phase with a higher boiling point, such as mineral oil, was selected for the continuous organic phase. The higher viscosity of the mineral oil relative to kerosene was also expected to be beneficial for rendering greater high-temperature stability to the emulsions. Furthermore, it was also hoped that this higher viscosity would suppress extensive agglomeration of the solid particles.

The stability and other characteristics of these mineral oil emulsions were presented in a previous section. Emulsions were evaporated by a procedure similar to that used with kerosene-based systems, but higher evaporation temperatures were employed. The influences of individual variables on powder morphology were studied by varying one experimental condition while keeping the others constant at so-called standard values. The standard procedure is defined as emulsion composition of 70% mineral oil; 25% aqueous 0.44M $Y(NO_3)_3$; 5% Arlacel 83 prepared by 15 minutes sonic treatment, with evaporation carried out at 240°C in a nitrogen purge atmosphere. Precursors following toluene washing and centruging calcined at 1000°C for several hours to produce yttria powders.

Electron micrographs of yttria powders obtained by the standard procedure are shown in Figure 7. The particles are spherical in shape rather narrow in size distribution typically ranging from 1 to 3 μm in diameter. There appears to be some agglomeration but individual morphology of the particles is retained. Some of the particles appear to be hollow.

Influence of evaporation temperature on the particle size distribution of yttria powders obtained by evaporation of the standard emulsion composition is shown in Figure 8. Particle size distributions obtained at temperatures lower than 200°C were excluded from the figure, as these powders showed extensive agglomeration and thus exhibited a wide size distribution. As the

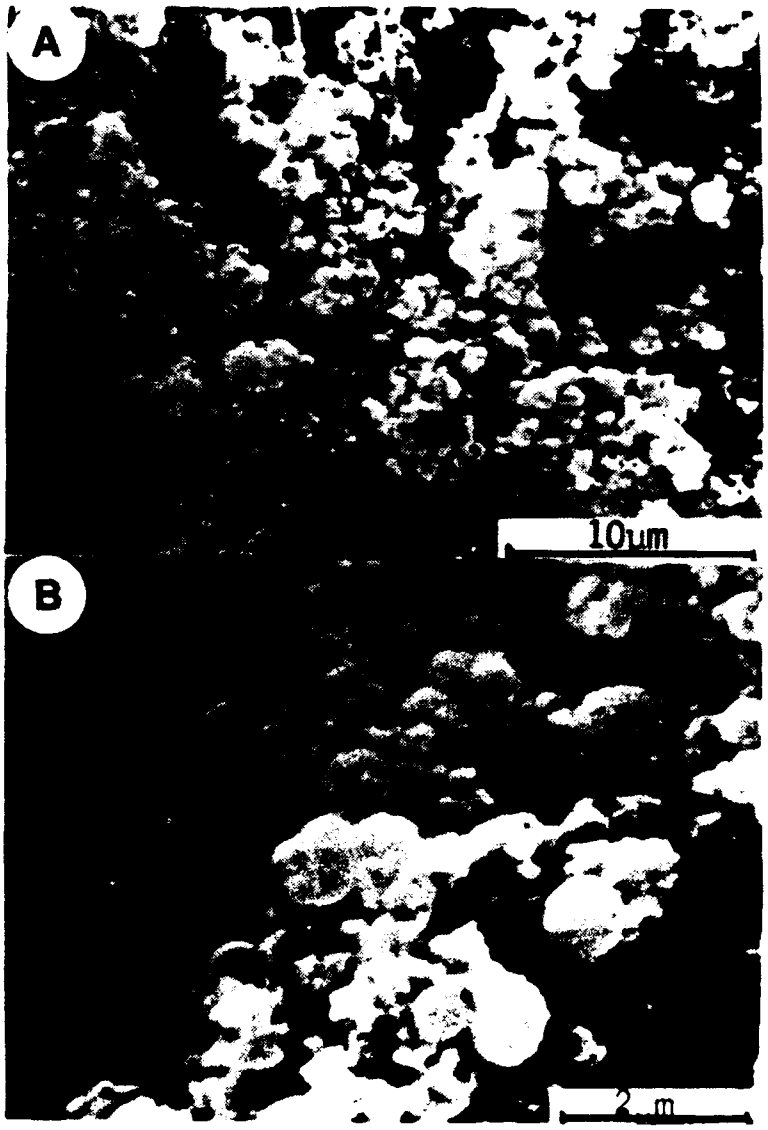

Fig. 6. Scanning electron micrograph of yttria powders derived from evaporation of w/o type emulsions. (73% kerosene, 25% aqueous 0.44 Y^{+3} solution and 2% Arlacel 83 evaporated at 180°C.)

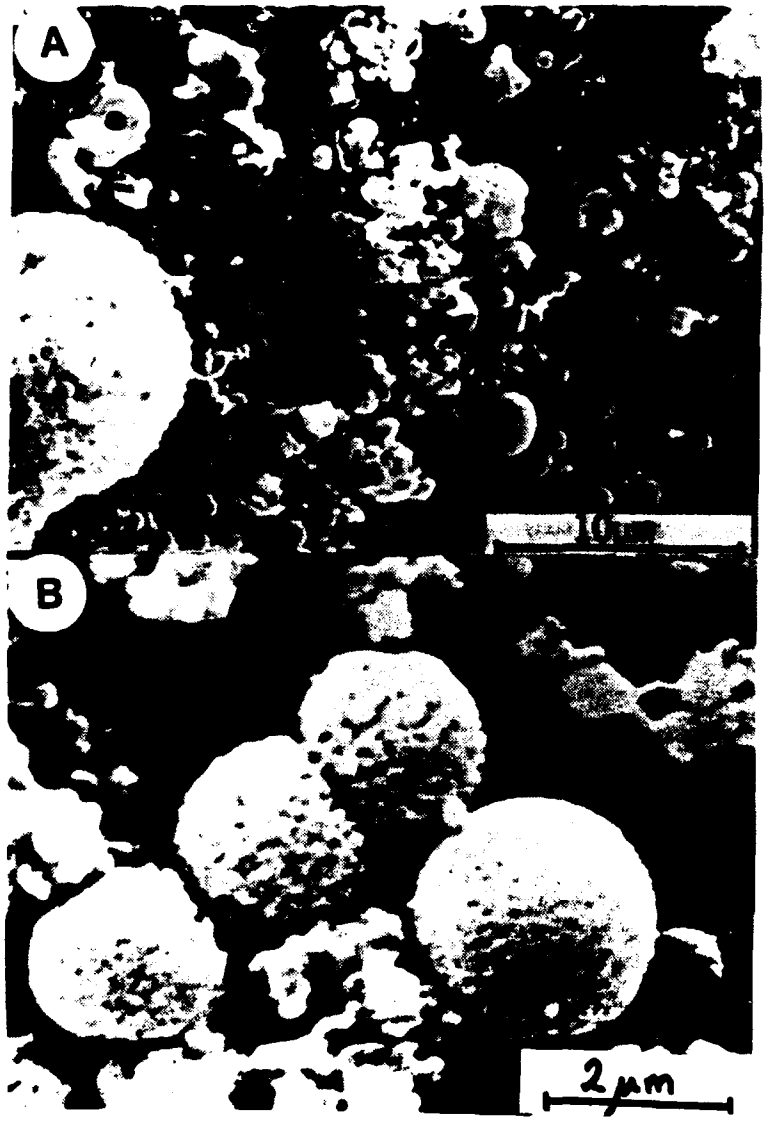

Fig. 7. Scanning electron micrographs of powders obtained from evaporation of 70% mineral oil, aqueous 25% 0.44M Y^{+3} solution, 5% Arlacel 83 emulsion. Evaporation was carried out at 240°C in N_2 atmosphere.

figure indicates the distribution is bimodal at 200°C (suggesting agglomeration); however, increasing the temperature not only eliminates the agglomerates but also shifts the peak to smaller sizes. No significant reduction in particle size is observed above 230°C, with the mean particle size of powders in the 230-250°C range being around 1.5 μm. The variation of median particle size with evaporation temperature in various atmospheres is shown in Figure 9. In all three atmospheres, a general trend of decreasing median particle size with increasing evaporation temperature is observed. In all cases studied, the median particle size ranges between 3 and 1 μm. Although vacuum appears to produce smaller median size than the other two atmospheres the actual size distributions were wider in the cases of vacuum atmosphere. Powders prepared in an air atmosphere were similar to those produced with nitrogen purge up to 220°C; above that temperature, the median size showed higher values for air than nitrogen atmospheres. It was observed that the evaporation rate of water became high enough at 230°C that water vapor was not effectively removed from the reactor in a static air atmosphere, and it condensed back into the oil bath, causing excessive oil hydrolysis. This was thought to cause agglomeration of the powders produced.

After studying the influence of evaporation temperature and atmosphere on the particle size, it was decided that 240°C and nitrogen purge were optimum conditions for these variables.

The influence of emulsifier concentration on the particle size distribution is shown in Figure 10. In these experiments the emulsifier concentration was varied between 1 and 10% of the total emulsion volume, while the organic-to-aqueous phase ratio was kept constant at the standard value of 2.8. The results were as expected, i.e., increasing the emulsifier concentration caused particle size distributions to shift to smaller sizes. The effect is most apparent between 1 and 4% emulsifier. While the distribution becomes narrower and the peak shifts toward smaller sizes when the emulsifier concentration is increased from 6 to 10%, the changes are not all that significant. Thus, a 5% emulsifier concentration was considered to be optimum for this system.

The influence of yttrium ion concentration on the powder morphology was studied by increasing the yttrium ion concentration from the standard level of 0.5M up to 3.5M, which is close to the saturation limit. Variation of mean particle size and surface area with yttrium ion concentration are summarized in the following table:

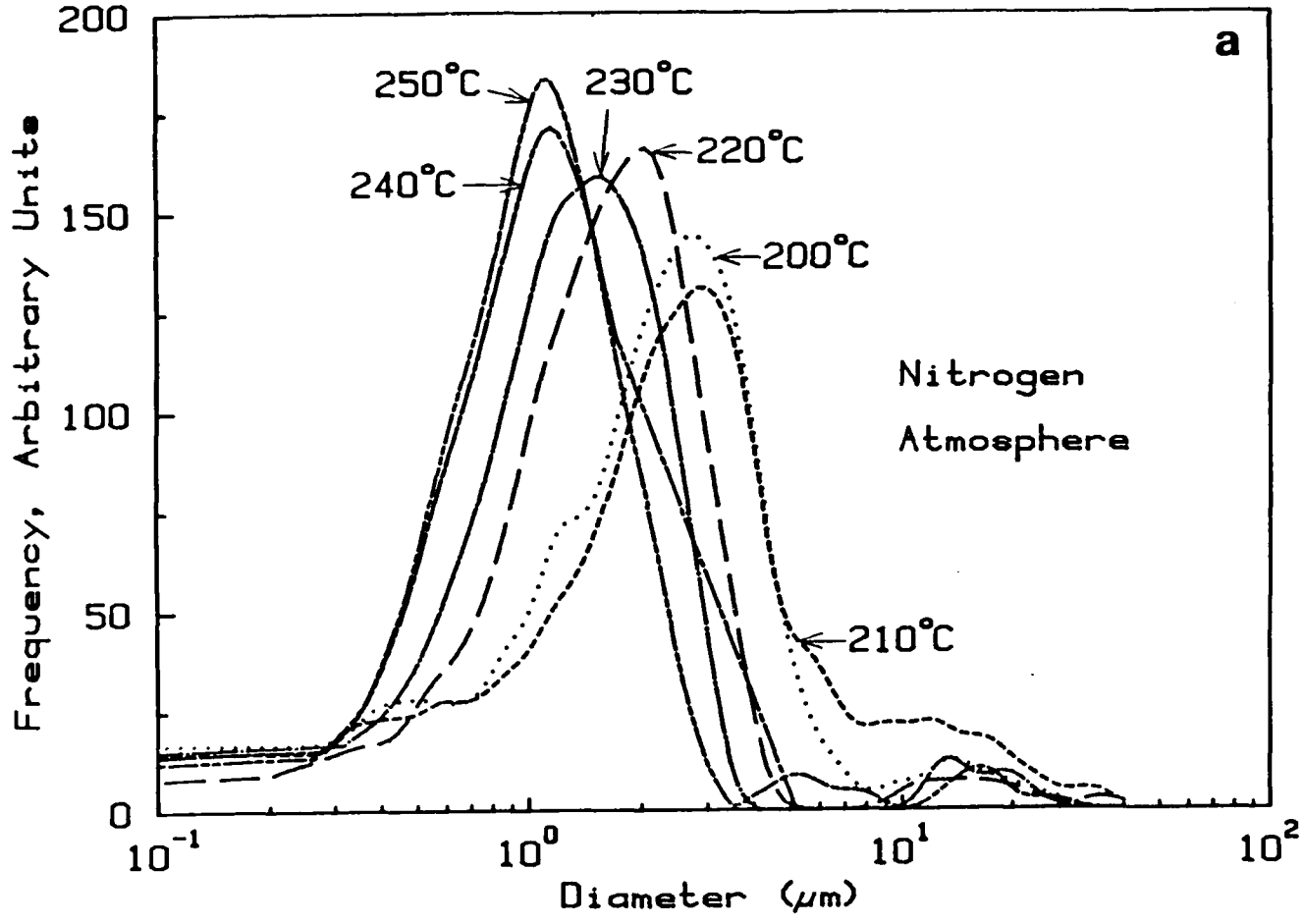

Fig. 8. Particle size distribution of yttria powders obtained from evaporation of mineral oil/$Y(NO_3)_3$/Arlacel 83 emulsions at various temperatures. Emulsion composition is 70% oil, 25% Aqueous phase and 5% Emulsifier in each case. a) nitrogen, b) vacuum c) air atmosphere.

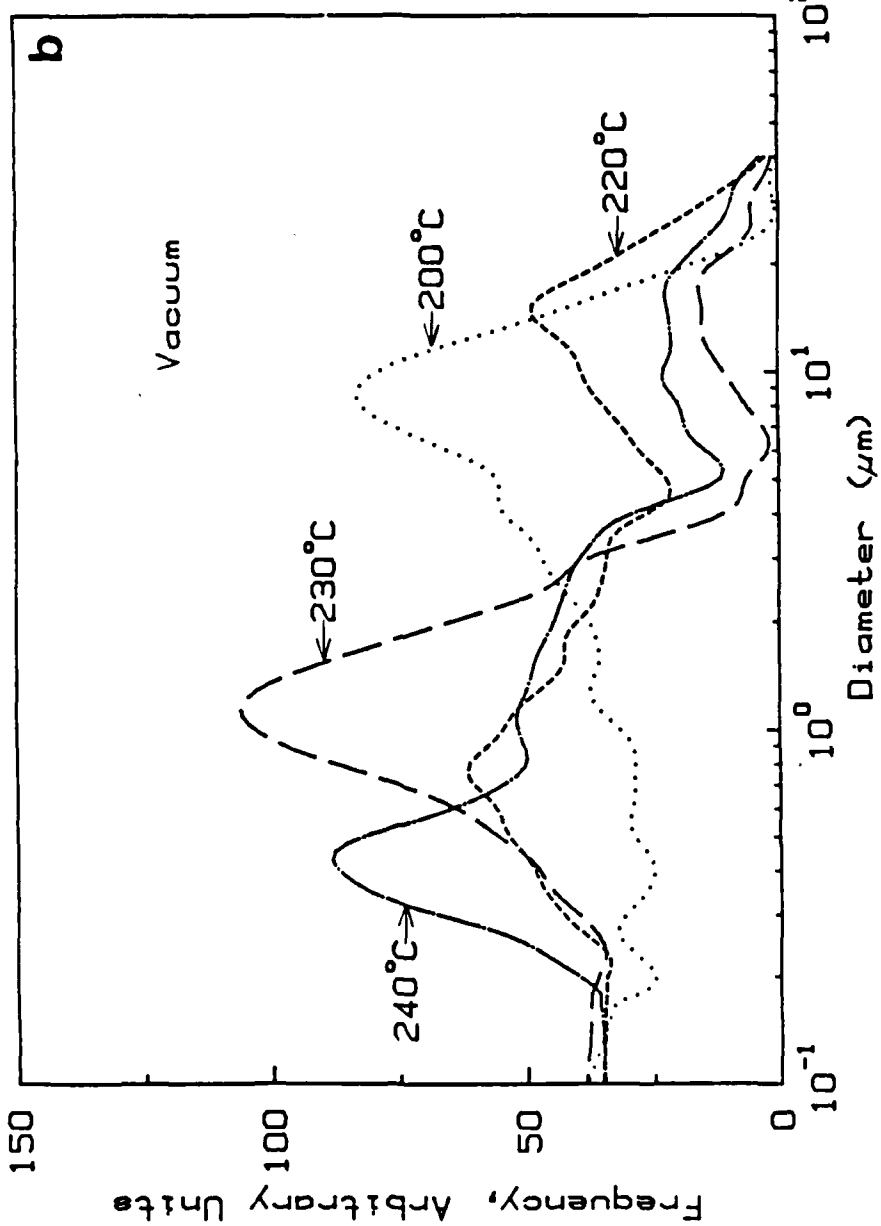

Fig. 8 (continued)

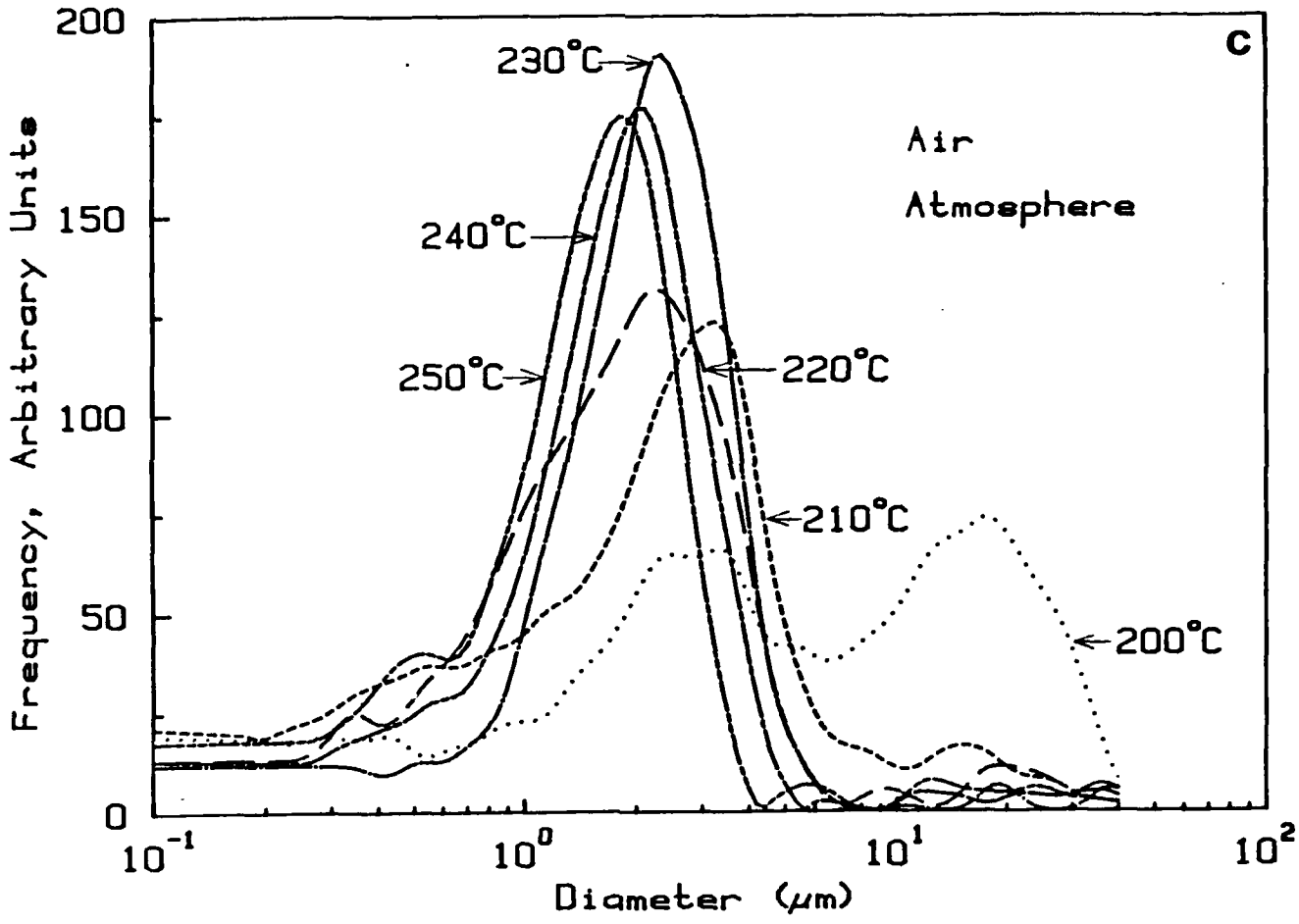

Fig. 8 (continued)

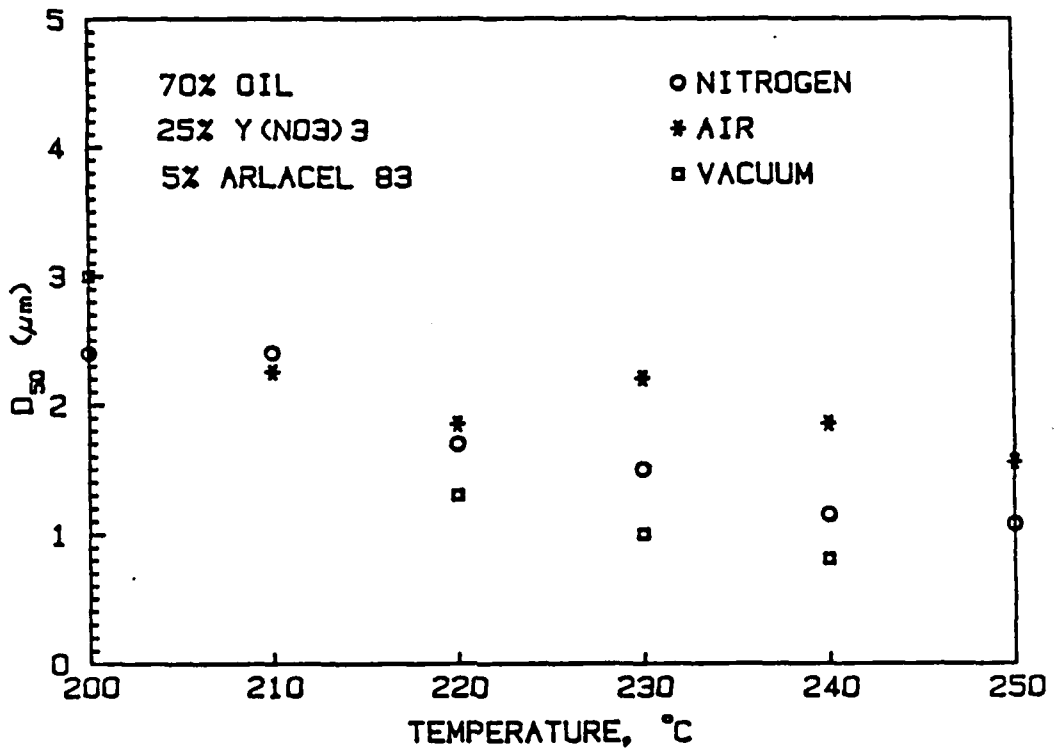

Fig. 9. Variation of median size, of yttria powders obtained by evaporation from mineral oil/$Y(NO_3)_3$/Arlacel 83 in various atmospheres.

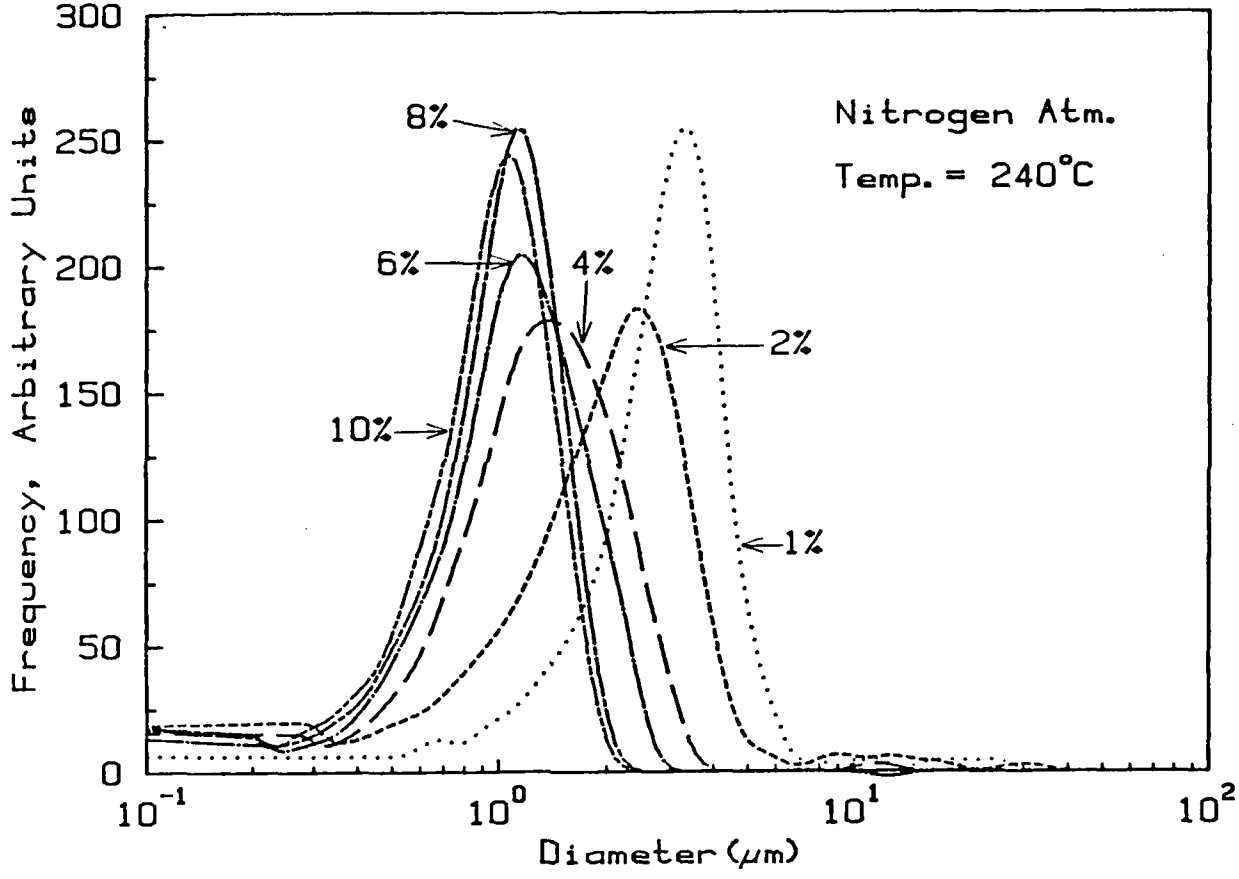

Fig. 10. Particle size distribution of yttria powders as a function of emulsifier concentration. In these experiments, mineral oil-to-aqueous phase ratio was kept constant at 2.8, and evaporation temperature was 240°C.

Table 3 - Influence of yttrium ion concentration on the powder characteristics produced by emulsion evaporation.

	Diameter, μm		Surface area, m^2/g		Yield,%
$[Y^{+3}]$,M	Precursor	Oxide	Precursor	Oxide	
0.5	4.3	1.5	8.4	4.9	84
1.0	5.0	1.6	10.4	5.2	86
1.5	3.8	2.2	24.7	4.5	84
2.0	4.9	2.5	20.3	4.2	84
2.5	5.6	2.3	15.8	3.6	87
3.0	6.0	2.7	6.8	2.7	85
3.5	8.9	3.7	3.9	2.7	86

Note: Precursors dried at 160°C, oxides calcined at 1000°C in air.

As the concentration of the yttrium ion is increased, mean particle size of both the precursor and the oxide increase, but only slightly. Similarly as the concentration of yttrium is increased, the specific surface area of the oxide powder decreases, but that of the precursor powder appears to go through a maximum at intermediate concentration. It is not clear whether such a maximum has any physical meaning or is caused by a small variation in the amount of organic residue left on the precursor. If a process is to be implemented on an industrial scale, it should yield relatively large quantities of powder per batch as well as have a high percentage of powder recovery. The yield of the process may be defined as the percent of Y_2O_3 recovered from what was introduced into the emulsion. From Table 3, it appears that the yield remains constant at 85 $\pm$ 2% over the concentration range studied. The small loss in product is believed to be due to incomplete recovery of the powder following evaporation. With improved washing and centrifugation processes, it is likely that the yield can be improved to near the theoretical value.

Results of these studies have shown that powders having a narrow size distribution with a mean diameter around one micron size can be produced reproducibly and relatively easily by emulsion evaporation from mineral oil. However, these results also raise two questions which remain unanswered. First, the emulsifier concentrations indicated in Figure 10 are far in excess of the amounts required for coverage of 1 μm aqueous droplets with a close-packed arrangement of surface active molecules, yet increasing the emulsifier concentrations up to 5% showed a significant change in the particle size distribution of the powders produced. Although no clear understanding is available for this discrepancy, a

plausible explanation may be offered if one considers the HLB value of the emulsifier. Arlacel 83 has an HLB value of 3.7 which favors w/o emulsions and yet it is completely soluble in the oil phase. It seems very likely that only a small fraction of the emulsifier is concentrated at the oil-water interface while most is dissolved in the oil phase. There is scientific and practical need for investigation of the distribution coefficients of the emulsifier in the oil and aqueous phase and at the interface. The other question is concerned with the size of the particles relative to the size of the droplets from which they are derived. The micrographs and particle size distributions indicate that the oxide particles obtained by emulsion evaporation were roughly the same size as the emulsion droplets. The particle size of solid oxide particles should be related to size of the emulsion droplet by (5):

$$D_{ox} = \left(\frac{C}{\rho_{ox}}\right)^{1/3} D_L$$

where D_{ox} and D_L are the diameters of the oxide particle and liquid droplet, respectively, C is the concentration of yttrium expressed as grams of Y_2O_3 per cm^3 and ρ_{ox} is the density of yttria (5.031 g/cm^3). For a one micron size droplet, with 0.44M Y^{+3} ion concentration in the solution, the diameter of the oxide particle should be around 0.2 μm. The discrepancy between the calculated and observed particle size may be due either to the particles not being solid (in which case the density of yttria used in above equation does not correspond to actual powder density), or to the larger-than-expected particles consisting of agglomerates of smaller primary particles. Either of these explanations is consistent with the limited experimental evidence available. Electron micrographs of powders at higher magnifications (see Figure 7b) indicate that at least some of the particles are indeed hollow. It is very likely that, when the aqueous droplet is heated rapidly in the hot oil bath evaporation starts from the surface to form a solid skin or shell the size of the original droplet. Further evaporation may occur through pore channels or cracks in this shell, giving a spongy appearance. This mechanism is illustrated schematically in Figure 11. The second mechanism involves initial formation of solid 0.2 μm primary particles followed by agglomeration of these particles in the hot oil bath with time to form larger (i.e. 1 to 3 μm) granules. Microscopic observations do not preclude this mechanism either. Indeed, close examination of micrographs shows that the larger spheres are collections of smaller primary particles of about 0.1 to

A) HOLLOW PARTICLE FORMATION

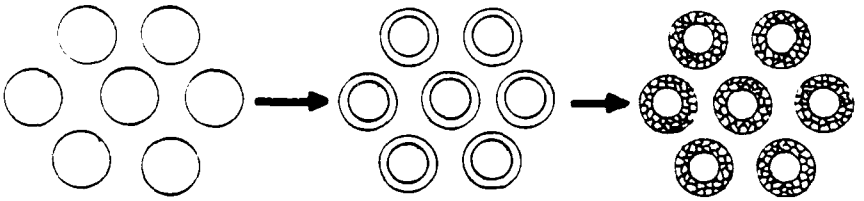

B) AGGLOMERATION

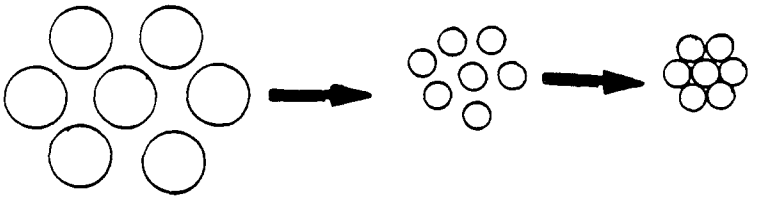

Fig. 11. Schematic representation of possible particle formation mechanisms in evaporation studies a) hollow particle formation b) agglomeration mechanism.

0.2 μm in size, thus favoring the second mechanism. At the present time there is not enough discriminating data to decide as to which mechanism is actually occurring under specific conditions. Further investigation into this problem is needed.

2.B.2. Emulsion Precipitation

Chemical precipitation of precursor particles from w/o type emulsions was investigated using light hydrocarbon liquids as the oil phase, aqueous 0.44M $Y(NO_3)_3$ solution as the water phase and a mixture of Span 60 and Tween 80 as the emulsifying agent. Although several organic liquids (including toluene, benzene, hexane) were studied, no significant difference was observed among them. Thus the major efforts in powder characterization and processing of powders were carried out with emulsions that employed toluene as the organic phase. The standard emulsion for these experiments was 72% toluene, 25% aqueous 0.44M $Y(NO_3)_3$, and 3% emulsifier (1.6% Span 60 + 1.4% Tween 80). Precipitation of precursor particles within the aqueous droplets was accomplished by adding an organic base to the emulsion with stirring and allowing it to diffuse into the droplets to cause precipitation. Among the organic bases investigated triethylamine, triethanolamine, tetrabutyl ammonium hydroxide, methylamine and pyridine were successful in producing precipitate (10). Inorganic bases such as ammonium hydroxide and sodium bicarbonate solutions also produced precipitates (11). The control of the precipitation reaction and therefore the particle morphology was difficult in the case of inorganic bases. The majority of the work reported in this section was carried out using either triethanolamine or ethylamine as the precipitating base.

Details of the precipitation and powder recovery procedures are discussed in a previous publication (10). The standard procedure involves addition of 20 ml triethanolamine to 600 ml standard emulsion (as defined above) with stirring, followed by addition of 1200 ml acetone to break emulsion and then centrifugation to recover the precipitate. Precipitate is dried at 100°C and calcined at 750°C to obtain yttria powders. Figure 12 shows the particle size distribution of the yttria powder obtained following the standard procedure. The distribution shows that particles have a size range of 0.2 to 2 μm with a peak around 0.6 μm. A scanning electron micrograph of the same powder is shown in Figure 13. The individual particles appear to be about 0.1 μm in size and are spherical, as anticipated. There appears to be some

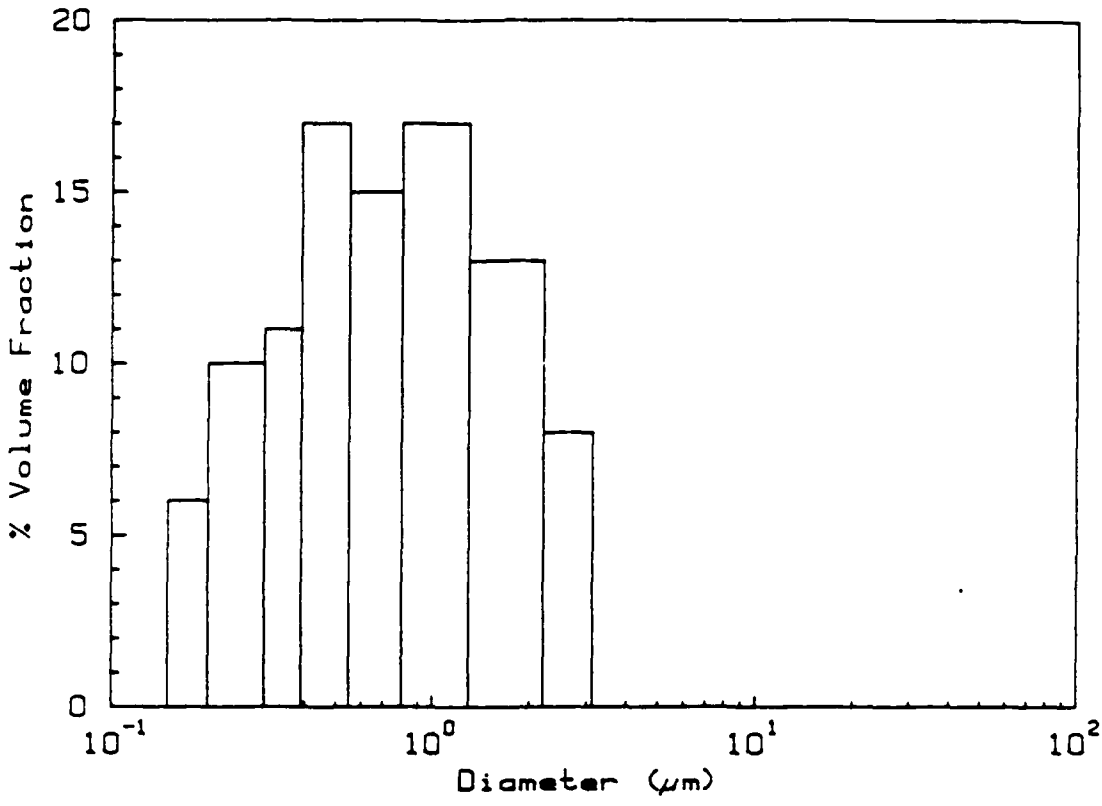

Fig. 12. Particle size distribution of powder obtained by emulsion precipitation using TEA as the organic base. Powder was calcined at 700°C and dispersed in water.

Fig. 13. Scanning electron micrograph of the yttria powder for which the particle size distribution is given in Figure 12.

agglomeration of these individual spheres to form 1 μm particles. This agglomeration may be responsible for the larger mean size and wider distribution observed in the particle size distribution measurements (Figure 12).

To investigate the diffusion of organic base into the aqueous phase and its reaction there with the cation, a series of experiments was carried out using the standard emulsion and triethanolamine (TEA) as the base. First, TEA was added to a two-phase (water-toluene) system with no emulsifying agent or yttrium ion present. The dependence of pH in the aqueous phase on the amount of TEA added to the toluene is shown in curve (a) of Figure 14. Curve (b) shows the same relationship in the presence of the emulsifying agent, but with no yttrium ions present. Curve (c) shows the variation of pH when acidic yttrium solution is the aqueous phase. In the yttrium-free cases, the two curves (a and b) are almost coincident up to 8 ml TEA addition. Both start from pH = 6.8, both jump to 10 with the first 2 ml addition of TEA, and both remain more or less constant up to about 10 ml. This abrupt increase in pH clearly indicates that TEA diffuses into the aqueous phase and dissociates according to its K_b value irrespective of the presence of the emulsifying agent. In other words, up to at least 8 ml TEA addition, the emulsifying agent does not seem to inhibit the diffusion of TEA into the aqueous phase, nor does it appear to react with TEA. However, for TEA additions of 12 ml or more, the pH of the emulsifier-containing system is lower than the emulsifier-free system. This suggests that, above 12 ml TEA additions, the emulsifier interacts with triethanolamine molecules, probably in a manner similar to a saponification reaction. When yttrium ions are present in the aqueous droplets (along with excess nitric acid), the initial pH of the aqueous phase is equal to 1.2. In this case, adding 0.5 ml of TEA elevates the pH to 5.4, and it reaches 7.0 at a 2 ml addition. It then increases rather slowly up to a 12 ml TEA addition. It should be noted that precipitation of yttrium hydroxide starts around pH = 6.5 and is practically complete at pH = 8 (1). This means that yttrium hydroxide begins to precipitate at 1 ml addition of TEA and should be completed at 4 ml TEA addition. The plateau at around pH = 8 is due to buffering of the solution by TEA in the presence of the yttrium hydroxide precipitate. The analogous plateau occurs around pH = 10 in the absence of yttrium.

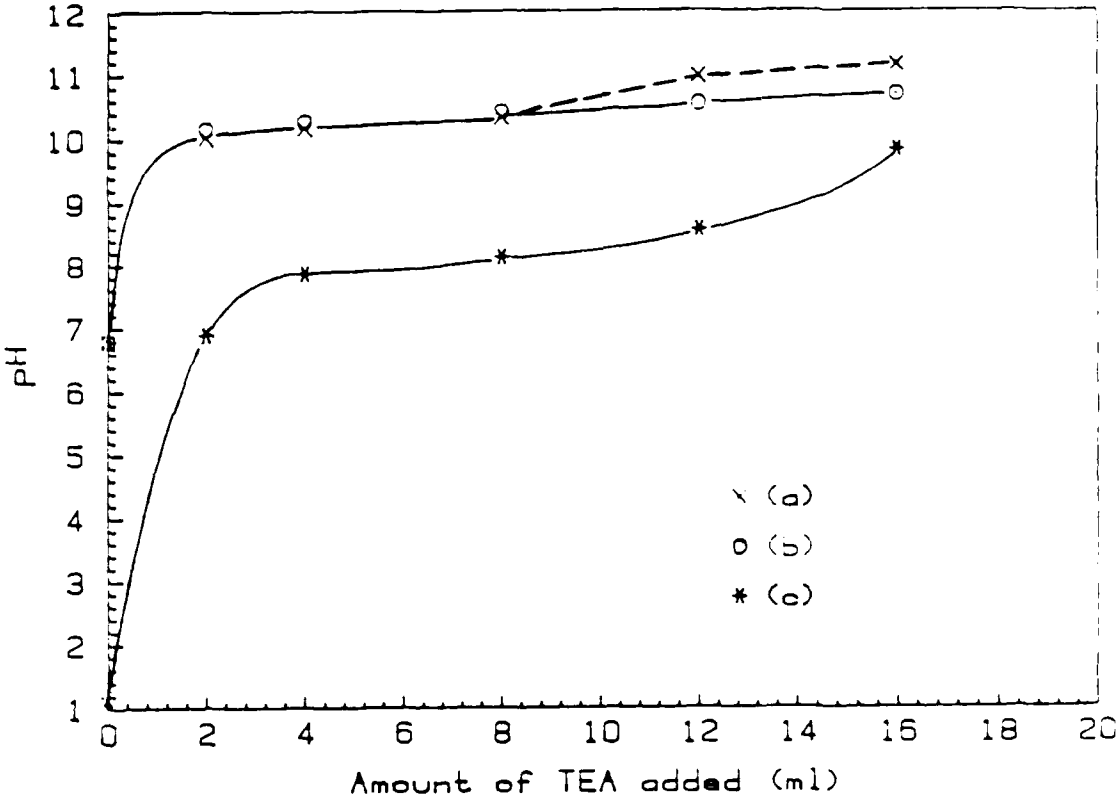

Fig. 14. Variation of pH in aqueous solution with the amount of TEA added to (a) toluene-water (no emulsifier, no yttrium ion); (b) emulsion of toluene-emulsifier-water (no yttrium ion); (c) emulsion of toluene-emulsifier-0.25 M Y^{3+} solution. The amount of TEA added is was for 150 ml of emulsions in (b) and (c). In (a) the 72%-to-25% ratio of toluene to water was preserved and 150 ml of the mixture was used.

3. CONSTITUTION

Precursor particles obtained by the emulsion evaporation process were brown-to-black in color and rather irregular in shape. Upon thermal decomposition the powders turned into white crystalline Y_2O_3. Spherical particle morphology was evident in electron micrographs of the oxide, as was discussed previously. These precursors showed a rather large but more or less constant loss on ignition (LOI) value of about 70% for a wide range of experimental conditions. Apparently, the precursors are not simple hydroxide or nitrate in but have a rather complex composition including some organic residue. Residue from a blank run (i.e. emulsion evaporation identical to the standard process except no yttrium ion in the aqueous phase) was analyzed for carbon, hydrogen and nitrogen along with one standard sample and one with an emulsifier concentration twice that of the standard. The results are shown in Table 4.

Table 4. Carbon, hydrogen and nitrogen analyses of selected precursors and blank run.

Composition	Carbon	Hydrogen	Nitrogen	%LOI
70.0% Min.Oil 25.0% $Y(NO_3)_3$ 5.0% Arl.83	38.305	3.955	3.525	70.71
66.3% Min.Oil 23.7% $Y(NO_3)_3$ 10.0% Arl.83	43.385	4.260	3.795	76.30
66.3% Min.Oil 23.7% H_2O+HNO_3 10.0% Arl.83	73.330	10.215	2.490	97.69

From the known constituents of the Arlacel 83, and assuming that the difference between the sum of C, H, and N values and the loss on ignition is due to oxygen in the residue, one can calculate the constitution of the residue from the blank run. Table 5 summarizes the results in terms of these components.

Table 5. Constituents of the blank run.

	Constituent %				
	Mineral Oil	Arlacel 83	NO_3	Ash*	Total
Carbon	63.66	9.67	---	---	73.33
Hydrogen	8.66	1.55	---	---	10.22
Nitrogen	---	---	2.49	---	2.49
Oxygen	---	3.12	8.53	?	11.66
Inorganics*	---	---	---	2.31	2.31
Total	72.32	14.34	11.02	2.31	100.00

*This is the ash after igniting the residue at 1000°C

Thus the residue of the blank run appears to be 72.3% mineral oil, 14.3% Arlacel 83, and 13.3% inorganic nitrates (See Figure 15). Obviously, the ash in the blank run (2.31%) was unexpected. Ignition of individual components has shown that the inorganics are associated with Arlacel 83 which originated as impurities introduced during the manufacturing of the emulsifier. Energy dispersive spectrometric analysis of the ash indicated that the majority of the ash was due to oxides of Si, Na, Al, K and Ca. Quantitative spectroscopic analysis of the contaminants at different concentrations of Arlacel 83 of yttrium ion are summarized in Table 6.

Table 6. Impurity analysis of the yttria powders produced by emulsion evaporation method

Sample #	$[Y^{+3}]$,M	Emulsifier Content, %	Impurity Content, ppm Na	K	Ca	Al
1	0.44	5	5600	76	37(?)	430(?)
2	1.0	5	2600	38	40	40
3	2.0	5	600	46	16	60
4	3.5	5	430	56	12	60
5	0.44	2	1200	53	333	150
6	0.44	10	27800	90	179	100

The table indicates that Na is the major impurity and that it apparently arises from the Arlacel 83. It appears that the K impurity also comes from emulsifier. The values for Ca and Al in Sample #1 are likely in error, since comparing the values in Sample #1 to those in 5 and 6 indicates that the actual value for Al in Sample #1 should be lower while that for Ca should be higher. It appears that the Ca and most of the Al comes from the Arlacel 83 as well. However, with the exception of Na, most of these impurities are insignificant, especially at higher yttrium ion concentrations. SiO_2 was analyzed by gravimetric methods. The standard sample showed about 200 ppm silica,

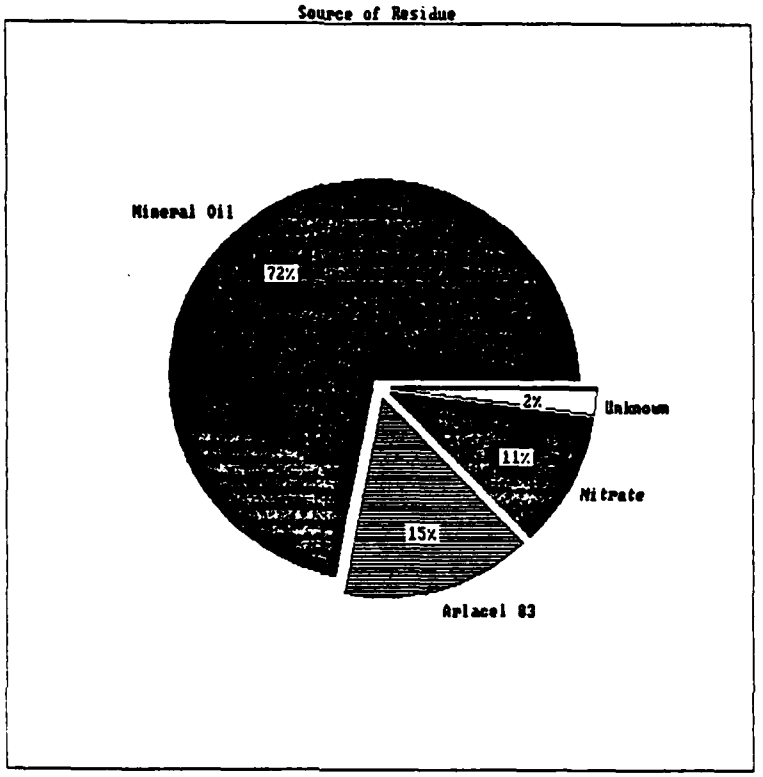

Fig. 15. Constitution of the residue from the blank run.

while at 3.5M Y^{+3}, the silica content was found to be about 1000 ppm. This result demonstrates that the silica impurity probably comes from the yttrium stock solution. Indeed, analysis of the as-received Y_2O_3 powder revealed 260 ppm SiO_2. Other impurities in the yttrium stock solution were found to be 80 ppm Na, 40 ppm K, <5 ppm Ca and 48 ppm Al. These results confirm that, with the exception of SiO_2, impurities found in the starting powder are insignificant compared to those introduced by the Arlacel 83. In future studies, a different nonionic emulsifier with low impurity content should be employed.

3.A. THERMAL DECOMPOSITION OF THE PRECURSORS

Chemical analysis of the precursors indicated that substantial amounts of organic residue remain in the precipitates. Thermal analyses of the precursor and a blank (organic residue without yttrium) were carried out to elucidate the nature of the precursor as well as the nature of the organic residue.

Differential thermal analysis of the precursor particles using a heating rate of 2°C/minute in an air atmosphere revealed three exothermic peaks (Figure 16). The first two peaks at 290°C and 395°C were easily discernable for all of the precursors analyzed. The third exothermic peak at 470°C, however, was clearly discernable only at higher Arlacel 83 concentrations and at higher sensitivities (see insert the Figure 16). Control experiments using a blend of Y_2O_3 powder, mineral oil and Arlacel 83 produced DTA patterns that were very similar to those produced by the residue-containing precursors, (Figure 17). Increasing Arlacel 83 contents in these control blends increased the intensity of the peak at 470°C while the others remained essentially unchanged. These control runs suggested that the first two peaks are associated with the oxidation of mineral oil, while the third peak is due to the oxidation of Arlacel 83. The absence of any endothermic peaks was surprising, since decomposition of a precursor (hydroxide, nitrate, carbonate or any of their combinations) to oxide would have produced an endothermic peak and a corresponding weight loss. Absence of such an endothermic peak may be attributed to several reasons: i) the precursor particles were actually a physical mixture of yttrium oxide and an organic residue, ii) yttrium formed an organometallic compound with the organic phase during evaporation which then oxidized rather than decomposed, or iii) an endothermic reaction occurred, but its presence was masked by one of the exotherms associated with oxidation of the organic phases.

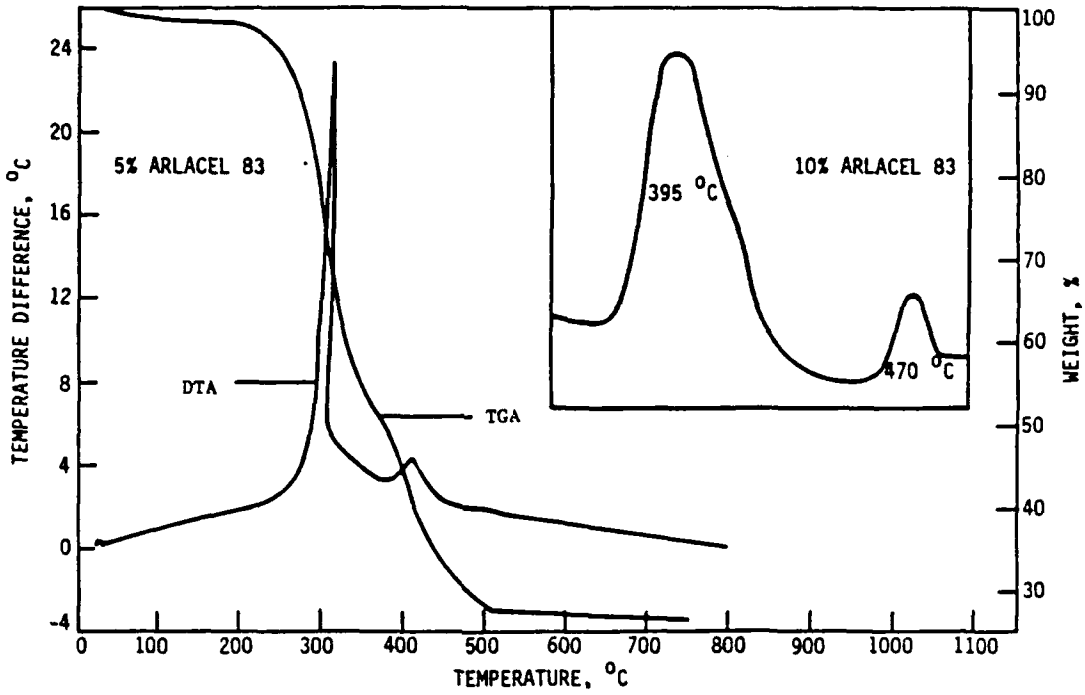

Fig. 16. TGA/DTA traces of standard precursor powder heated at a 2°C/min. in air. Insert: Portion of DTA trace of a powder produced from an emulsion with 10% Arlacel 83.

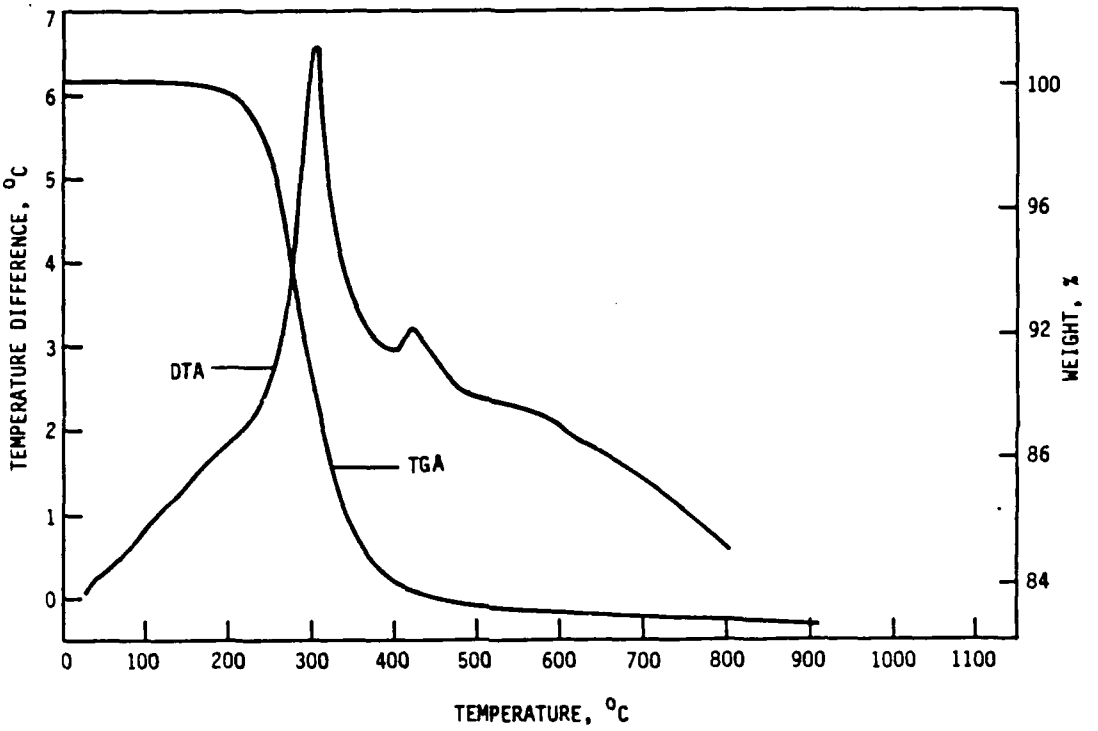

Fig. 17. TGA/DTA traces of a control sample prepared by mixing standard amounts of Y_2O_3, mineral oil and Arlacel 83.

Yttrium hydroxide and hydroxynitrate show at least two endothermic peaks upon heating in an air atmosphere, one in the 330-360°C range corresponding to partial dehydroxylation, and the other in the 520-570°C range corresponding to dehydroxylation and denitration (12). Since endothermic effects at these temperatures would not be masked by the exotherms observed in our precursors, it is unlikely that the precursors are simple hydroxide or hydroxide-nitrate salts. Recently, hydroxycarbonates of yttrium have been synthesized and characterized (13). Thermal decomposition of these powders in air show two major endothermic peaks, one around 200°C and one at 670°C. Since no 670° endothermic peak was observed with the precursors prepared in this study, it is unlikely that they consisted of a hydroxycarbonate or a simple carbonate. Since the powders were prepared at temperatures <250°C, it is also unlikely that the powders obtained were a simple mixture of oxide and mineral oil.

Infrared absorption spectra of the precursors from standard emulsion evaporation procedure following heat treatment at various temperatures are shown in Figure 18. The precursor dried at 110°C shows a large number of peaks. The broad peak around 3350 cm^{-1} and the shoulder at 1620 cm^{-1} are due to OH stretching and bending respectively (14). The sharp peaks at 2924 and 2854 cm^{-1} represent stretching frequencies for C-H bonds. The weaker peaks at 1458 and 1385 cm^{-1} are assigned to the stretching of C-C and C=C bonds (14). The peaks observed at 1566, 1317, 1028 and 814 cm^{-1} are believed to be due to nitrogen-oxygen stretching and bending, while the peaks at 1510, 1420, 1113 and 746 are due to carbon-oxygen bond stretching and bending (15). This spectrum indicates that the precursor powder contains a significant quantity of organic residue (apparently from mineral oil), some carbonate species as a result of oxidation and/or hydrolysis of mineral oil during evaporation, and nitrate which originates from the aqueous phase of the emulsion. At 350°C, all of the peaks that represent the C-H, C-C and C=C bonds are gone, indicating that the organic residue is already decomposed or oxidized . All of the peaks arising from NO_3 are also absent at this temperature. The peak due to OH stretching (~3335 cm^{-1}) becomes shallow. The powder resembles a carbonate material at this stage as $CO_3^{=}$ peaks are enhanced while the other peaks are either absent or reduced in intensity. Elimination of organic material at this temperature agrees well with the TGA/DTA results, which show a strong exotherm with an accompanying weight loss around 300°C (see Figure 16). Heat treatment at higher temperatures causes elimination of peaks due to OH and $CO_3^{=}$ and the development of Y-O absorption peaks at 561 and 467 cm^{-1}, which are typical of Y_2O_3. At 1000°C, only a small peak at 1437 cm^{-1} due to $CO_3^{=}$ is discernible

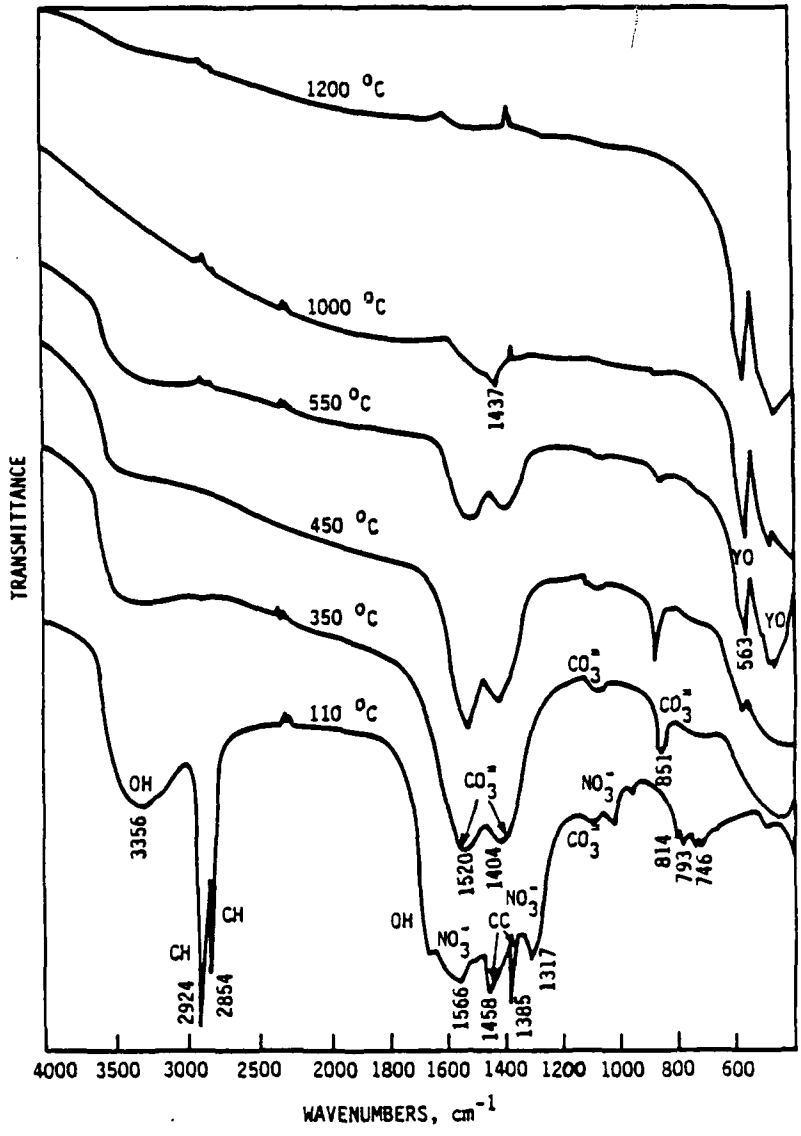

Fig. 18. Fourier transform infrared spectra of yttria precursors following heat treatment for 4 hours at various temperatures.

which is completely absent at 1200°C.

Infrared spectra of precursor powders obtained by emulsion precipitation were not significantly different from those of the emulsion evaporation powders. Powders showed C-H stretching peaks at 2922 and 2853 cm^{-1} which were eliminated above 300°C. Peaks associated with hydroxide and/or water around 3458, 1547 and 1447 cm^{-1} showed reduction in their intensity as the heat treatment temperature was increased. The peak at 1385 cm^{-1}, which was assigned to nitrate stretching, followed the same characteristics as hydroxyl peaks, but was completely absent at 700°C. Characteristic Y_2O_3 peaks at 561 and 465 cm^{-1} appeared around 600°C.

In general, these observations suggest that the precipitates produced by both methods are probably hydroxynitrates (12) combined with organic residue. Upon heating, precursors decompose to form first carbonate than oxide over a wide temperature range.

3.B. SINTERING BEHAVIOR

This work has shown that small, spherical particle yttria powders can be produced by emulsion techniques. Since the objective of this project is to produce powders suitable for the fabrication of ceramics, an important part of their characterization is to pack and sinter these powders and compare their sintering behavior to that of as-received powder. For these tests, compacts were prepared by first using biaxial dry pressing at 12 MPa followed by isostatic pressing at 207 MPa. Compacts were sintered in a vacuum furnace at at a range of temperatures and times. The sintering schedule was as follows: heating to 1000°C at a rate of 50°C/hr, a soak at 1000°C for one hour, heating to sintering temperature at a rate of 50°C/min, a soak at the sintering temperature (T_s) for a specified period of time followed by cooling to (T_s-200) at a rate of 50°C/min. Fast heating and cooling rates to and from sintering temperature were used to minimize sintering during heating and cooling steps. Bulk densities of the unsintered compacts were determined from geometric measurements and sintered densities were determined using a liquid immersion technique with toluene as the immersion liquid (16).

3.B.1. Sintering of Powders from Emulsion Evaporation

Relative unfired bulk densities of the yttria compacts were 49.42 ± 0.38% and 57.75 ± 0.44% for the

emulsion derived (EP) and the as-received raw (RP) powders, respectively. These values were obtained from sample sizes of 60. The total pore volume for an EP compact obtained from mercury porosimetry gave a calculated relative sintered density of 52.5%, while that for a RP compact was 63.8%. The higher calculated densities from porosimetry measurements are probably due to i) the inability of mercury to penetrate into closed pores, and ii) an increase in density during the porosimetry measurement due to the application of a higher isostatic pressure than was used during compact pressing (the maximum applied pressure was 515 MPa in porosimeter tests as compared to 207 MPa for isostatic pressing). The pore size distribution for the two different unsintered powder compacts is shown in Figure 19. The EP compact showed a symmetrical distribution with a peak at 0.05 μm. The pore radius calculated for random packings of 1 to 3 μm diameter granules gives a range between 0.08 and 0.62 μm, which is almost completely outside (above) the measured pore size distribution for EP. Packing of 0.1 to 0.2 μm diameter primary crystallites, however, gives a calculated pore radius ranging from about 0.01 to 0.04 μm, which corresponds to the lower half of the distribution shown in Figure 19. Apparently, the observed pore radius is dominated by packing of the primary crystallites yielded by breakdown of the agglomerates, but the actual packing is probably more open than the random packing of uniform spheres assumed in the calculations. Observations of a fracture surface of the EP compact following isostatic pressing has shown that the majority of the granules have been broken down into a matrix of primary crystallites with only a few granules retaining their morphology. Presence of these intact granules, however, does not create pores with large openings, because there is no continuous network of intact granules.

The relative sintered densities of the EP and RP compacts as a function of time and temperature are given in Figure 20. In the 1500°C series and the three shortest sintering times in the 1600°C series, the RP compacts sintered to a higher relative density than the EP compacts. For all the remaining temperature/time combinations, the EP compacts exhibited higher sintered densities. The higher densities of the RP compacts at the lower temperature are most likely due to the higher green density of the unsintered RP compacts. RP compacts had an unsintered relative density about 10% higher than that of the EP compacts. The EP compacts appear to have a significantly higher densification rate than the RP compacts. For instance, a relative density of 0.9 was achieved in 3, 15 and 135 minutes at 1800, 1700 and 1600°C for EP compacts, whereas it required about 70 minutes at 1800°C and was not achieved even after 150 minutes at 1600

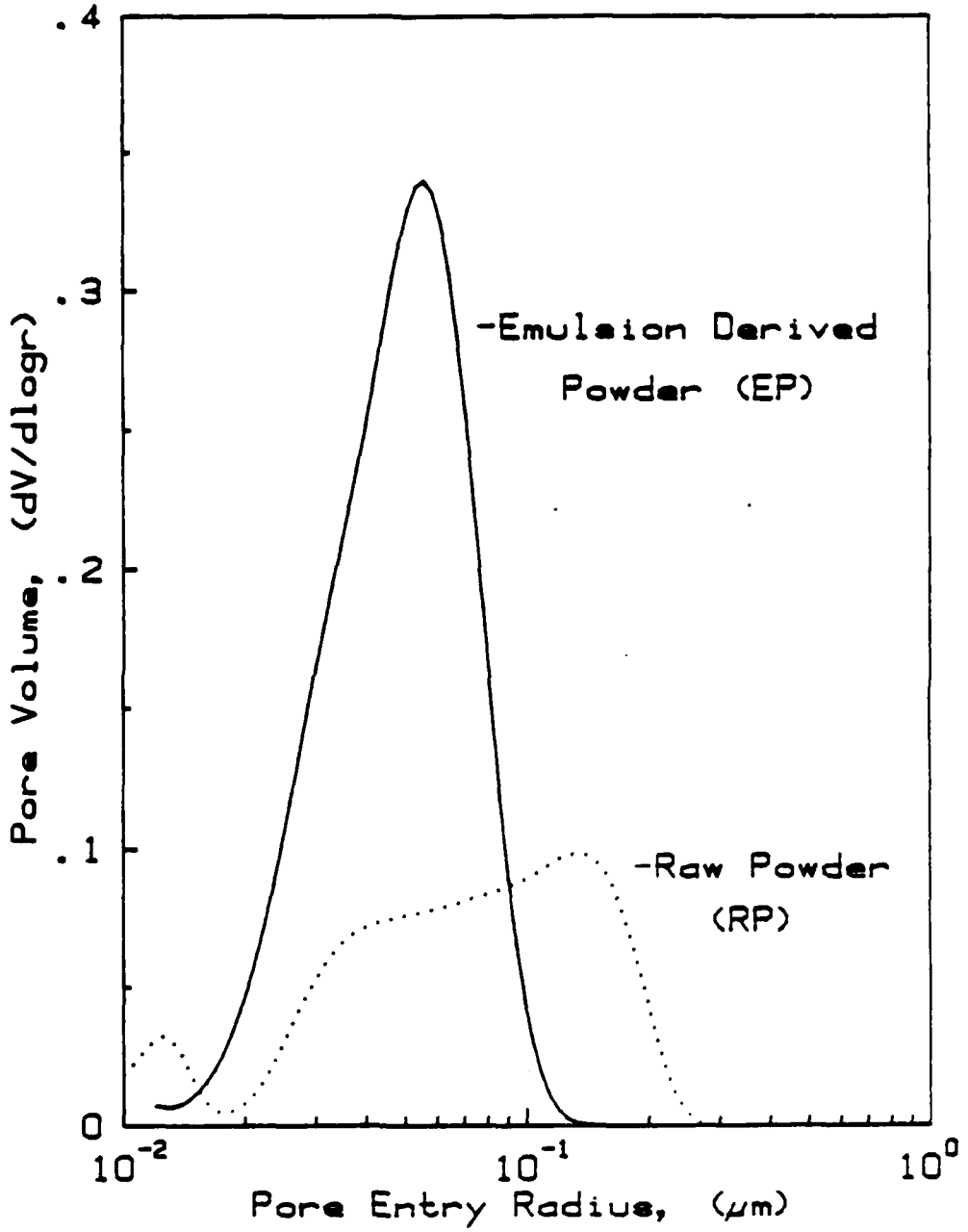

Fig. 19. Pore entry radius size distribution obtained from mercury intrusion porosimetry for compacts of emulsion derived (EP) and raw (RP) powders.

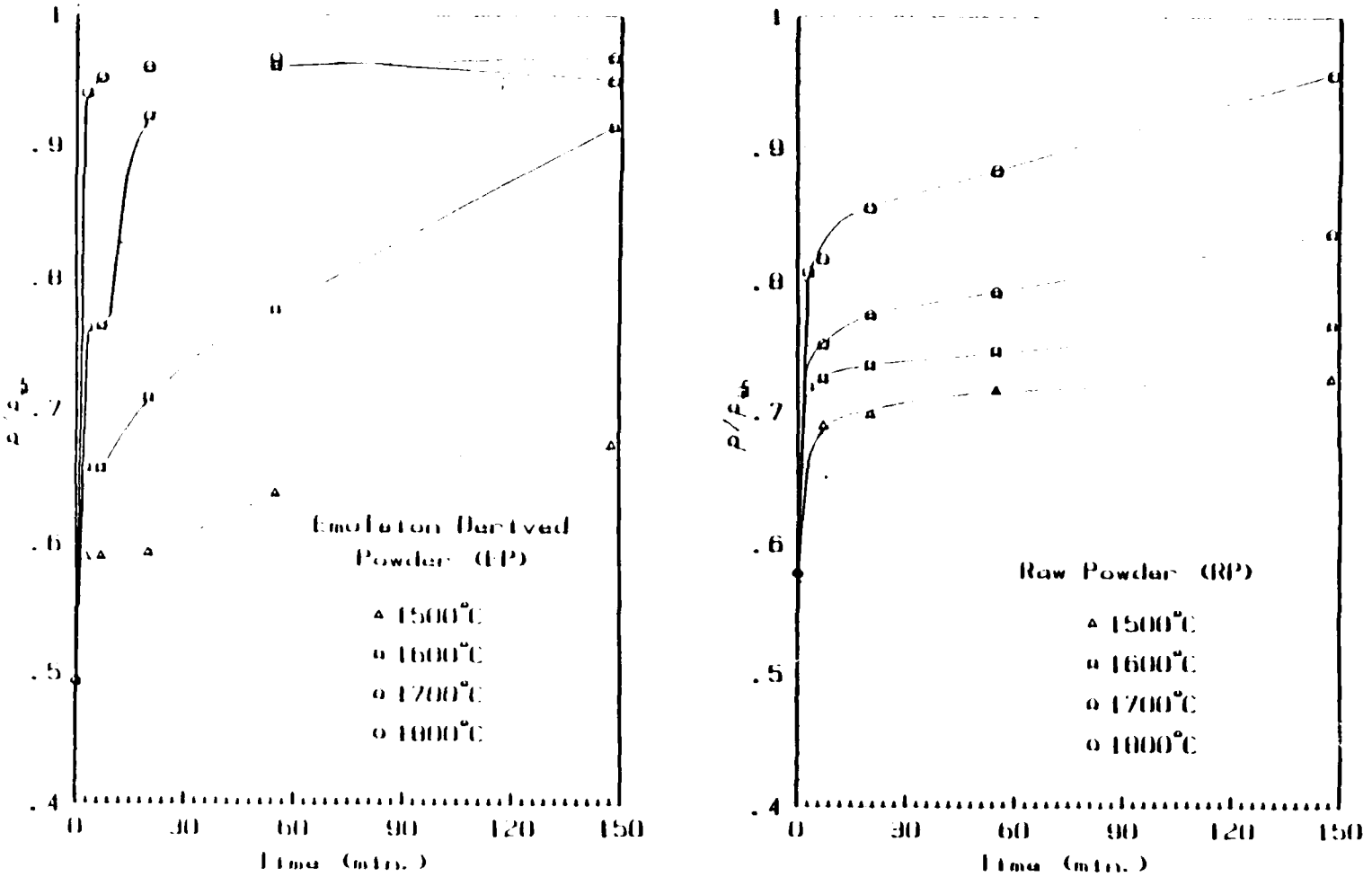

Fig. 20. Relative density, ρ/ρ_{th}, as a function of time for EP and RP compacts at isothermal conditions.

and 1700°C for RP compacts.

An interesting feature of the sintering behavior of the EP compacts not observed for the RP compacts was the apparent densification delay between 3 and 20 minutes in the 1500°C series, and between 3 and 7 minutes in the 1600°C and 1700°C series. A possible explanation for this observed rate decrease may be found in the peculiar morphology of the emulsion derived particles. As discussed previously, the EP powder was made up of spherical granules which in turn were composed of a collection of 0.1-0.2 μm primary crystallites. These primary particle assemblies would be expected to sinter together at a rate much faster than a packing of the granules would.It is likely that the observed initial density increase was due to rapid sintering together of these primary particles. The density of the compacts then remained relatively unchanged until sufficient matter transport had occurred to allow the formation of significant necks between intact granules and the grains formed from the sintered primary particles.

The development of emulsion derived compact microstructure with respect to time at 1700° and 1800°C is shown in Figures 21 and 22. Initial stage sintering is evident in Figure 21a. At this stage significant neck growth has already occurred with an interconnected network of open porosity. An interesting observation is that hollow granules are discernible in the sintered matrix as spherical cavities with an average size of about 2 μm. (See upper right corner of micrograph in Figure 21a.) Figure 21b shows the transition between initial and intermediate stage sintering at which pores become more or less isolated yet are still located at the grain boundaries. It appears that most of the densification occurs until the porosity is pinched off into isolated closed pores at the grain intersections (see Figure 21c). The last micrograph in Figure 21 shows that grain growth has become the dominant process leaving pores within the grain interiors. At this stage further densification becomes very difficult, due to long diffusion paths for vacancies to reach grain boundaries. Figure 22 shows that final stage sintering has begun after only 3 minutes at a sintering temperature of 1800°C. Apparently initial and intermediate-stage sintering are completed during heating to the sintering temperature. An interesting observation in this figure is that the last micrograph shows cracks in the microstructure. Apparently this is caused by rapid cooling from the sintering temperature. Since the grains are large, thermal shock causes internal cracking.

Variation of grain size as a function of sintered density for the EP compacts is shown in Figure 23. This plot reveals that grain size at a specific relative density is independent of sintering temperature, which is

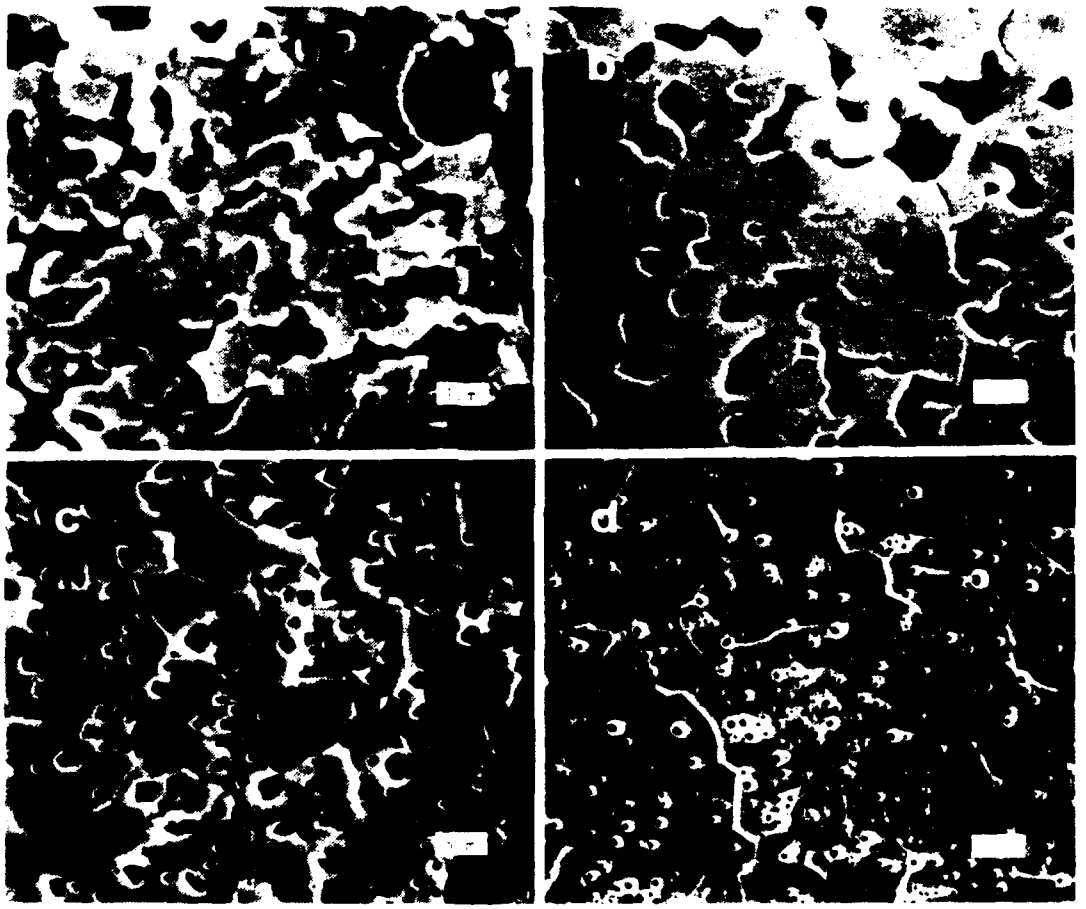

Fig. 21. Scanning electron micrographs of polished and etched surfaces of EP compacts sintered at 1700°C for a) 3, b) 7, c) 20 and d) 148 minutes.

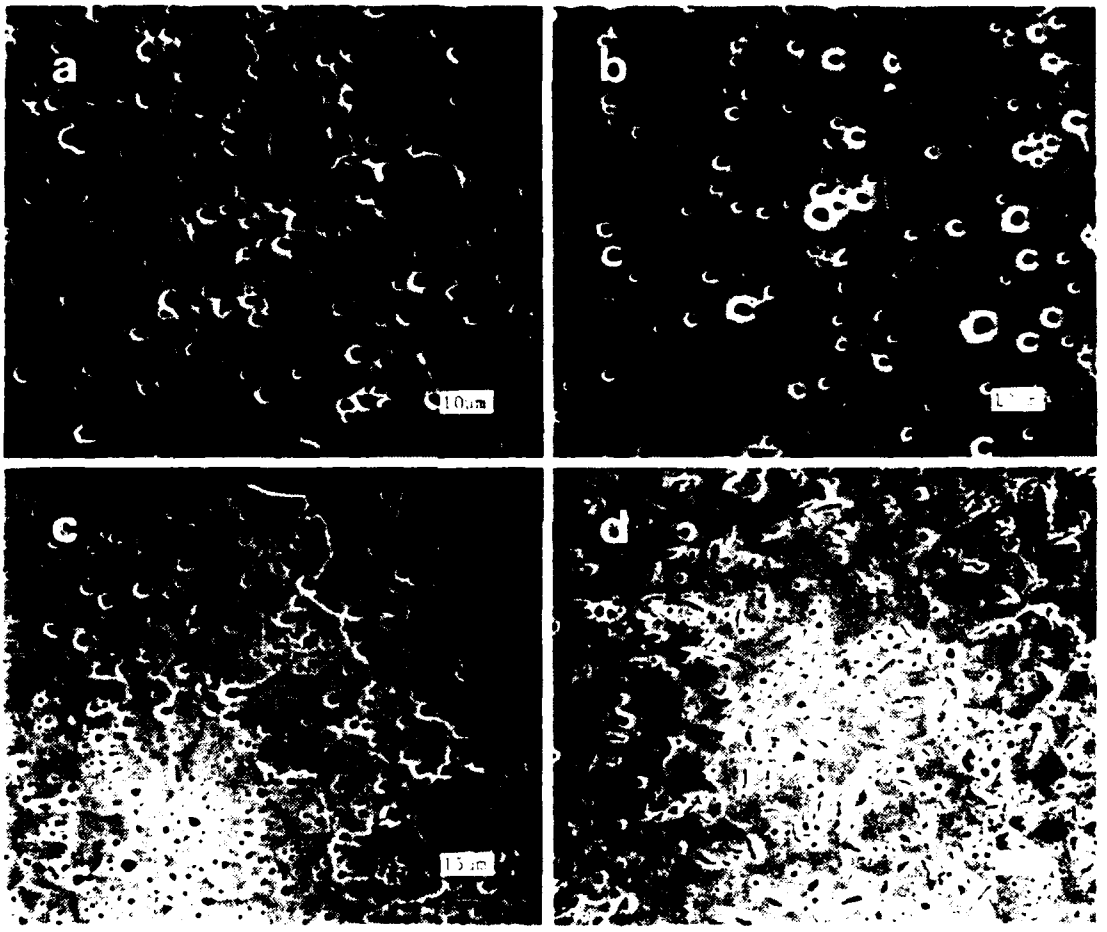

Fig. 22. Scanning electron micrographs of polished and etched surfaces of EP compacts sintered at 1800°C for a) 3, b) 7, c) 20 and 55 minutes.

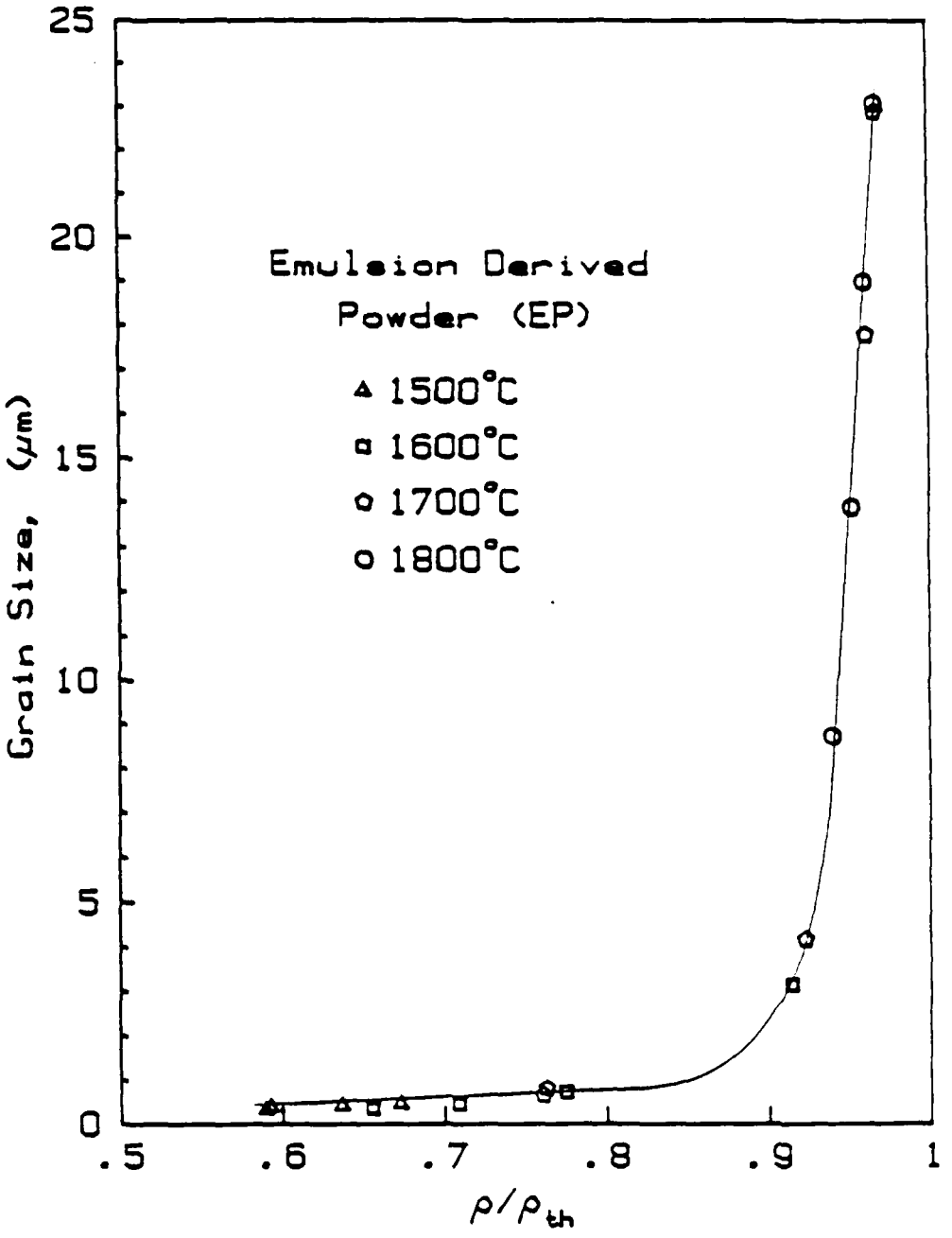

Fig. 23. Variation of grain size with relative sintered density at various sintering temperatures.

in agreement with results reported by Barringer et al. (17). Figure 23 and the photomicrographs in Figures 21 and 22 show that very little grain growth occurred until the relative density reached approximately 0.91, but was very rapid above that density. Barringer et al. (17) reported that rapid grain growth began at a relative density of 0.93 for TiO_2 and Wang (from reference 17) found a value of 0.90 for Al_2O_3. This indicates that achievement of very dense microstructures requires the restraint of grain growth, and in particular, discontinuous grain growth initiating at low relative densities must be avoided.

3.B.2. Sintering of Powders from Emulsion Precipitation

Sintering experiments similar to those described in the previous section were carried out with powders that were obtained by the emulsion precipitation technique. Unsintered relative densities were found to be about 46%. Sintered densities as a function of time and temperature are shown in Figure 24. The sintering behavior of these powders was superior to that of any Y_2O_3 powder that has been synthesized in our laboratory or elsewhere, to the best of our knowledge. Even at 1500°C, sintered relative density exceeded 95% in 10 minutes. At long sintering times (12 hours) the relative density exceeded 99%. For 1600°C, a sintered density of 95% was achieved in 3 minutes and 99% in 5 hours. Finally at 1700°C, a sintered density of 99% was observed in 10 minutes. The density increased to 99.7 in 100 minutes at 1700°C, but decreased slightly at longer sintering times. The decrease in sintered density for these samples is believed to be due to cracks formed during quenching of these samples, as was described in the previous section.

The results of sintering of powders derived by emulsion precipitation are very exciting and suggest that this technique may have greater promise than the emulsion evaporation technique for producing high quality ceramic powders. In addition to evidence of extremely high sintering activities for these powders, the precipitation route avoids possible process complications introduced by emulsion residues in the precursors derived by evaporation and may therefore lend itself more readily to scale up to large volume production. The development and understanding of the emulsion precipitation technique is not as far along as the emulsion evaporation technique. Although the current contract has expired, the Engineering Research Institute at Iowa State University is temporarily supporting a single graduate student effort to continue the study of post-emulsion processing and characterization

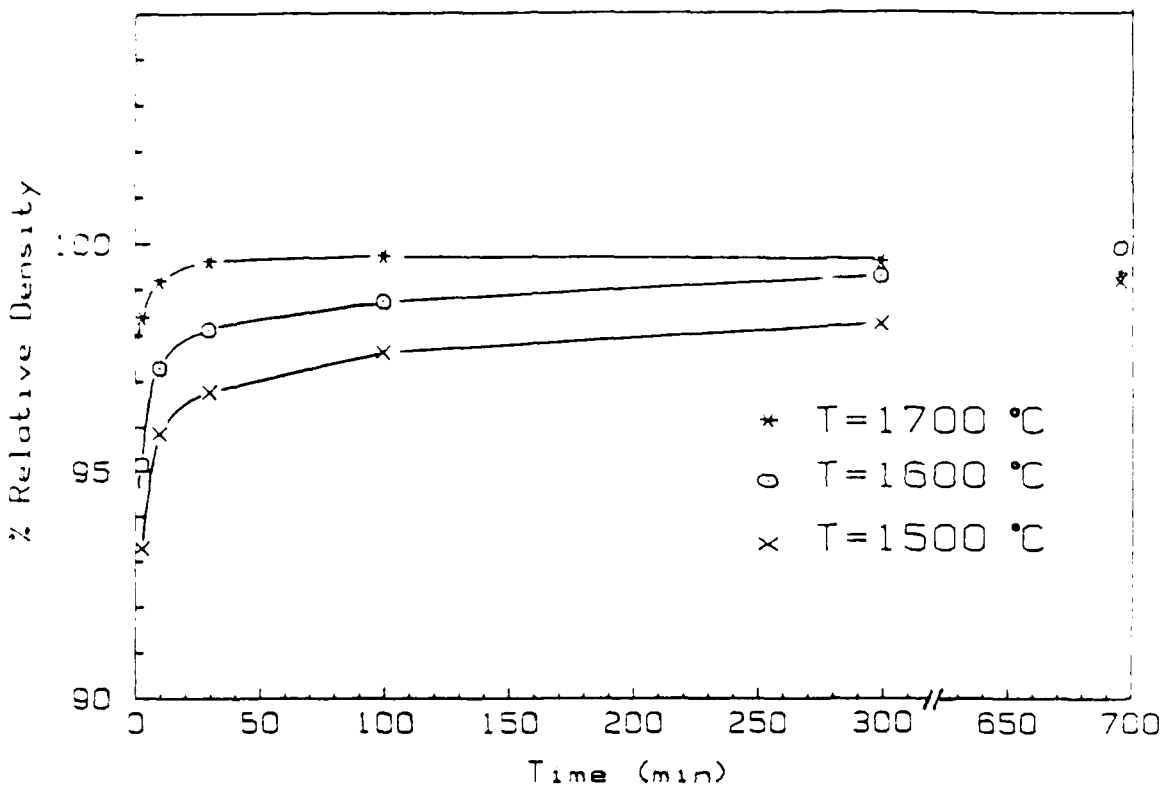

Fig. 24. Variation of sintered density with time for emulsion precipitated Y_2O_3 powder compacts at various temperatures.

of microstructures produced by sintering of powders derived by emulsion precipitation. Significant progress toward a basic understanding of this promising process and investigation of scale-up potential would benefit from an increased level of funding.

3.C. OTHER SYSTEMS

In addition to the preparation of yttria, which constituted our major effort in this program, preliminary work was undertaken on the preparation of powders of a number of other oxides considered to be important and used widely. These oxides included Al_2O_3, MgO and $MgAl_2O_4$. All three systems produced small particle size uniform powders by emulsion evaporation. Studies on the preparation of these oxides by emulsion precipitation is underway.

Figure 25a shows a micrograph of alumina powder obtained by the emulsion evaporation technique, indicating that the particles are spherical ranging from several microns up to 50 microns in diameter. The significant difference between the processing of this powder and that the yttria described above was that the alumina emulsion was prepared by mechanical stirring rather than by sonic disruption. Consequently, the alumina emulsion itself exhibited a rather large median droplet size and a wide size distribution, which resulted in a coarser size distribution in the powder produced. Figure 25b shows the morphology of magnesia powder produced by the emulsion evaporation method. Since this emulsion was sonicated, the particles produced were extremely small (~0.1 μm) but appeared to be somewhat agglomerated. A detailed investigation into emulsion stirring and its relation to powder particle size is needed. In particular, different agitation instruments as well as sonic disruption at various resonance frequencies to cover a broad range of droplet size for various systems needed to be investigated.

The morphology of spinel powder produced by emulsion evaporation is most interesting (see Figure 26). It appears that the particles have a bimodal size distribution: large spheres resembling those of alumina (fig. 25a) and small spheres similar to those of magnesia (Fig. 25b). However, energy dispersive x-ray analysis indicates that the compositions of all particles are uniform throughout and that both sizes of particles contain both magnesium and aluminum. The mechanism of particle formation and characterization of the these powders will be studied in the future.

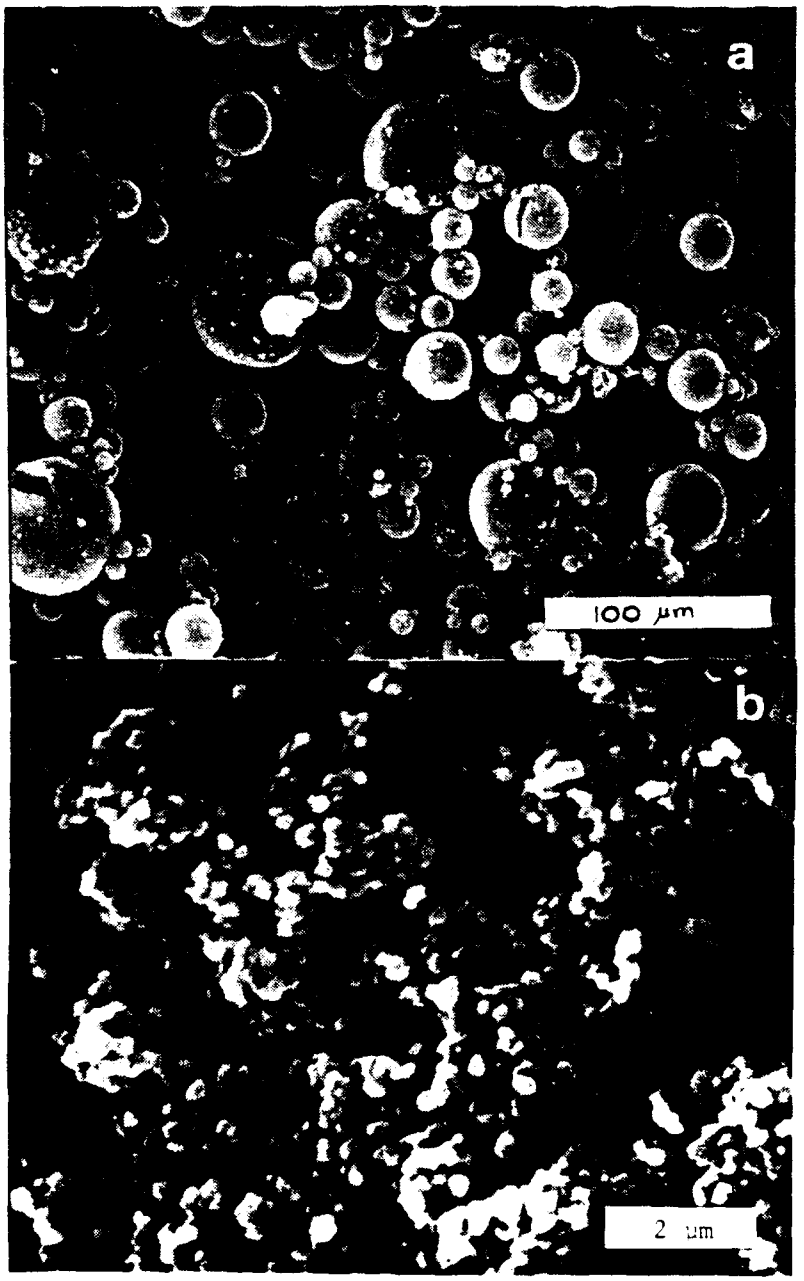

Fig. 25. Alumina (a) and magnesia (b) powders obtained by emulsion evaporation technique. Procedures were the same as the standard yttria procedure, except the emulsion was stirred mechanically for alumina and sonicated for magnesia.

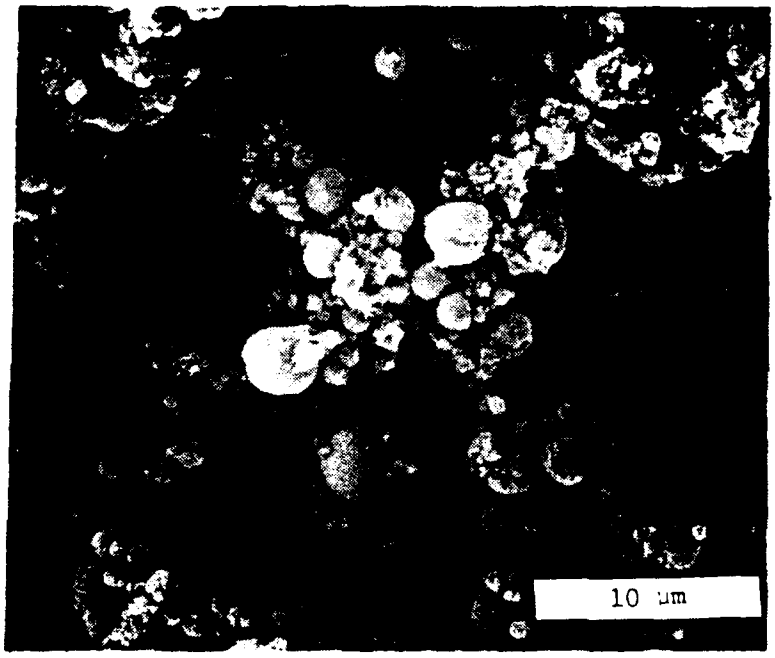

Fig. 26. Spinel powder obtained by the emulsion evaporation technique.

4. SUMMARY

A number of significant results have been obtained during the course of this investigation. The most important results can be summarized as follows:

i) Yttria granules of spherical shape and about 1.5 μm average particle diameter with a narrow size distribution (1 to 3 μm) can be produced reproducibly by the emulsion evaporation technique. The granules themselves consist of primary crystallites of 0.1 to 0.2 μm in size. (See Publication No. 1 and 2.)

ii) Yttria powders of spherical shape and nearly uniform submicron (~0.1 μm) size can be successfully produced by the emulsion precipitation technique. (See Publication No. 4 and 5.)

iii) The average particle size of the oxide powders can be controlled to a large extent by altering the emulsion droplet size and to a lesser extent by manipulating the cation concentration of the aqueous phase. Depending upon the emulsion preparation procedure, powders with an average particle size of 0.1 to 5.0 μm can be produced.

iv) Preliminary results show promise for other simple and complex oxides.

Finally, a result which is not scientific in nature but which is equally significant is that our emulsion processing research program has drawn worldwide attention. Overall interest in our techniques and program has been very satisfying. It is the understanding of the author that groups at MIT, Sandia National Laboratory, The Pennsylvania State University and a group in Japan have already initiated research following along the lines of our work.

5. LIST OF PUBLICATIONS

1. Mufit Akinc and Kerry Richardson, "Preparation of Ceramic Powders from Emulsions", pp. 99-109 in Mat. Res. Soc. Symp. Proc. Vol 73 Better Ceramics through Chemistry II. J. Brinker, D. Clark and D. Ulrich eds. MRS. publ. 1986.

2. Kerry Richardson and Mufit Akinc, "Preparation of Spherical Yttrium Oxide Powders Using Emulsion Evaporation", Ceramics International (Accepted).

3. Kerry Richardson and Mufit Akinc, "Sintering of Yttrium Oxide Powders Prepared by Emulsion Evaporation", Submitted to Ceramics International, April 1987.

4. Mufit Akinc and A. Celikkaya, "Preparation of Yttria Powders in Emulsion Precipitation" to appear in Advanced Ceramic Science, Proceedings of the Powder Science and Technology Symposium, August 1-4, 1986, Boston, MA.

5. Ahmet Celikkaya and Mufit Akinc, "Preparation and Characterization of Oxide Powders by Emulsion Precipitation", in preparation.

6. LIST OF SCIENTIFIC PERSONNEL PARTICIPATED IN THE PROJECT

1. Mufit Akinc, Ph.D., Associate Professor, Principal Investigator
2. Kerry Richardson, B.S., Graduate Research Assistant
3. Ahmet Celikkaya, M.S., Graduate Research Assistant
4. Daniel Sordelet*, B.S., Graduate Research Assistant

*Supported in part by this project.

Daniel Sordelet and Kerry Richardson have finished their studies and have received Master of Science degrees. Ahmet Celikkaya is working toward his Ph.D. and is expected to complete his degree requirements by Fall of 1988.

7. REFERENCES

1. M. D. Rasmussen, G. W. Jordan, M. Akinc, O. Hunter, Jr. and M. F. Berard, "Influence of Precipitation Procedure on Sinterability of Y_2O_3 Prepared from Hydroxide Precursor," Ceramics International 9 [2], 59-60, 1983.

2. S. L. Dole, R. W. Scheidecker, L. E. Shiers, M. F. Berard and O. Hunter, Jr., "Technique for Preparing Highly-Sinterable Oxide Powders", Mat. Sci. & Engr. 32, 277-81, 1978.

3. M. D. Rasmussen, M. Akinc and O. Hunter, Jr., "Processing of yttria powders derived from hydroxide precursors", Ceramics International, 11 (2), 51-55 (1985).

4. W. H. Rhodes, "Agglomerate and Particle Size Effects on Sintering Yttria-Stabilized Zirconia", J. Am. Ceram. Soc. 64 [1].

5. M. Akinc, Preparation Fine Oxide Powders by Emulsion Precipitation, proposal submitted to ARO, February, 1984.

6. M. Akinc, Progress Report #1 submitted to ARO December 1985.

7. a) P. Becher, Emulsions: Theory and Practice, 2nd edition, Reinhold, New York, 1965.
   b) Philip Sherman, Ed., Emulsion Science p 149, Academic Press, London 1968.

8. K. Shinoda and H. Kunieda, in Encyclopedia of Emulsion Technology, edited by Paul Becher (Marcel Dekker, New York, 1983), pp. 337-367.

9. M. Akinc and K. Richardson, "Preparation of ceramic powders from emulsions," Proceedings of the Materials Research Society Symposium, Better Ceramics Through Chemistry pp. 99-110, J. Brinker, D. E. Clark and D. R. Ulrich eds. MRS, Pittsburgh 1986.

10. M. Akinc and A. Celikkaya, "Preparation of yttria powders by emulsion precipitation", Proceedings of the American Ceramic Society Meeting on Powder Science and Technology (to be published).

11. M. Akinc, Progress Report #2 submitted to ARO, June 1986.

12. C. E. Holcombe, "Cementitious Yttria Products", Oak Ridge Y-12 Plant Report #Y2110, March 1978.

13. D. J. Sordelet and M. Akinc, "Preparation of Spherical Monosized Y_2O_3 Precursor Particles", J. int. Coll. Sci. (in press).

14. L. M. Seaverson, S. Q. Luo, P. L. Chen and J. F. McClelland, "Carbonate Associated with Sol-Gel Processing of Yttria: An Infrared Spectroscopic Study, J. Am. Ceram. Soc., 69(5) 423-29, (1986).

15. C. H. Rochester, "Infrared Studies of Powder Surfaces and Surface-adsorbate Interactions Including the Solid-liquid Interface: A Review." Powder Technology 13, 157-176 (1976).

16. K. Richardson and M. Akinc, "Preparation of Spherical Yttrium Oxide Powders Using Emulsion Evaporation", Ceramics International (in press).

17. E. A. Barringer, R. Brook, H. K. Bowen in Sintering and Heterogeneos Catalysis, edited by G. C. Kuczynski, A. E. Miller, G. A. Sargent (Plenum Press, New York, 1984), pp. 1-21.

8. ACKNOWLEDGEMENTS

The principal investigator acknowledges the support of Dr. A. Crowson, the Scientific Officer from the U.S. Army Research Office, throughout the course of this contract. Appreciation is expressed to Dr. M. F. Berard for his invaluable contributions to this project. The author thanks his assistants, Kerry Richardson and Ahmet Celikkaya, who worked long hours and endured the frustrations of research under my supervision.

END

12-87

DTIC